ACS OMEGA

http://pubs.acs.org/journal/acsodf

Review

Review of Polymeric Biomimetic Small-Diameter Vascular Grafts to Tackle Intimal Hyperplasia

Rumbidzai Zizhou, Xin Wang, and Shadi Houshyar*

Cite This: *ACS Omega* 2022, 7, 22125−22148

Read Online

ACCESS | Metrics & More | Article Recommendations

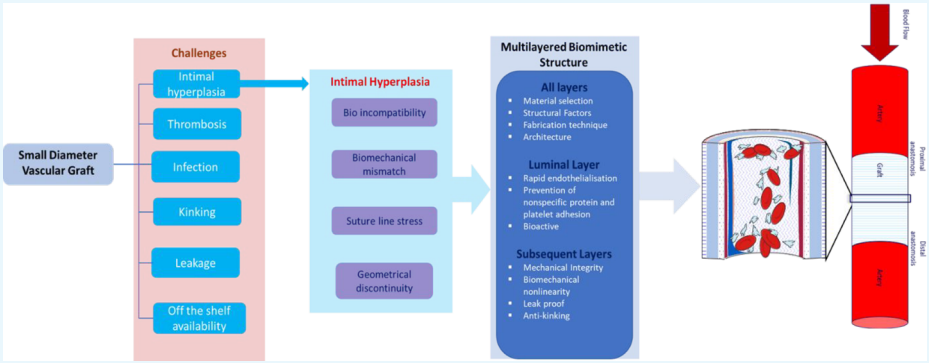

ABSTRACT: Small-diameter artificial vascular grafts (SDAVG) are used to bypass blood flow in arterial occlusive diseases such as coronary heart or peripheral arterial disease. However, SDAVGs are plagued by restenosis after a short while due to thrombosis and the thickening of the neointimal wall known as intimal hyperplasia (IH). The specific causes of IH have not yet been deduced; however, thrombosis formation due to bioincompatibility as well as a mismatch between the biomechanical properties of the SDAVG and the native artery has been attributed to its initiation. The main challenges that have been faced in fabricating SDAVGs are facilitating rapid re-endothelialization of the luminal surface of the SDAVG and replicating the complex viscoelastic behavior of the arteries. Recent strategies to combat IH formation have been mostly based on imitating the natural structure and function of the native artery (biomimicry). Thus, most recently, developed grafts contain a multilayered structure with a designated function for each layer. This paper reviews the current polymeric, biomimetic SDAVGs in preventing the formation of IH. The materials used in fabrication, challenges, and strategies employed to tackle IH are summarized and discussed, and we focus on the multilayered structure of current SDAVGs. Additionally, the future aspects in this area are pointed out for researchers to consider in their endeavor.

1. INTRODUCTION

Occlusive disease of the popliteal artery or more distal vessels requires bypassing with an autogenous vein to the distal popliteal artery or tibial vessels. The greater saphenous vein, an autologous blood vessel, remains the clinical gold standard.[1,2] Repairing diseased blood vessels using autologous vessels has many advantages, such as good tissue compatibility, no risk of immune reaction, matching mechanical properties, and good long-term patency. However, a good-quality autologous vessel is unavailable for many patients requiring surgery due to a previous harvest, anatomical variability (varying internal diameter, wall thickness, or compliance), or disease progression. Moreover, harvesting the vessel causes secondary trauma, which is not always available.[3,4] Due to the limited availability of autologous vessels, the far from ideal synthetic conduits, including expanded polytetrafluoroethylene (e-PTFE, Gore-Tex), polyethylene terephthalate (Dacron, PET), and polyurethane (PU),[5,6] are thereby used. Long-term patency has been achieved in grafts with diameters greater than 6 mm. Nonetheless, for smaller-diameter blood vessels, such as the femoropopliteal and tibial arteries found in the lower limbs, these materials have significant drawbacks, including infection due to technical mismanagement, thrombosis due to the lack of remodeling and growing capabilities of living tissues, and the development of intimal hyperplasia leading to restenosis of the graft.[2,7−9] Apart from autologous vessels and synthetic conduits, other prosthetic grafts include homologous grafts obtained from cadavers or donors such as

Received: March 22, 2022
Accepted: June 3, 2022
Published: June 21, 2022

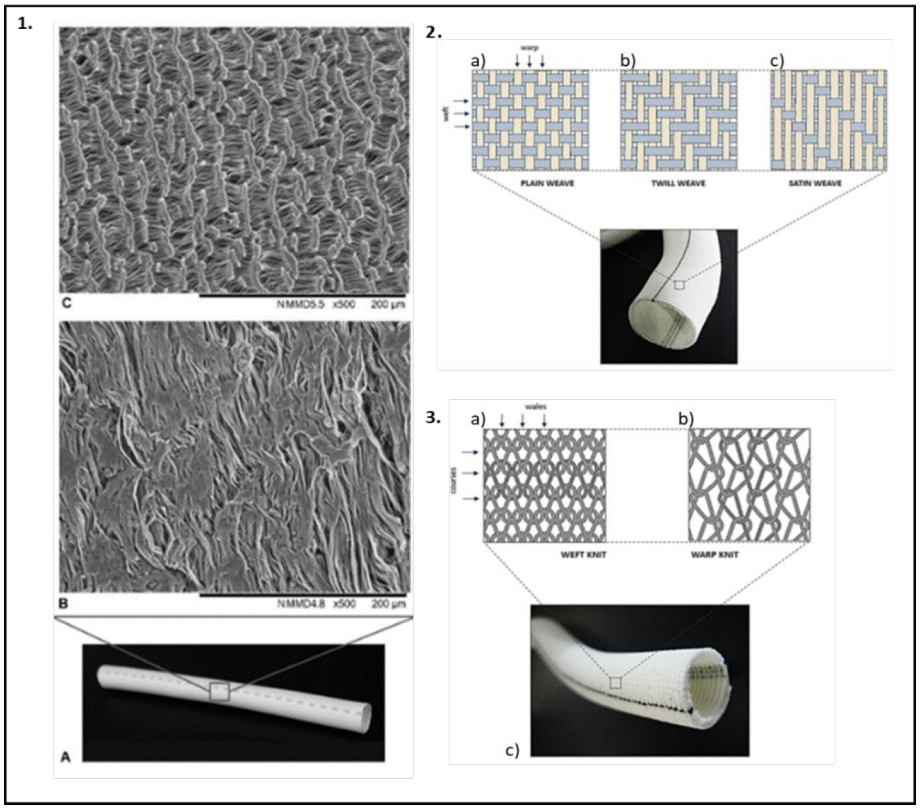

Figure 1. (A) Image of ePTFE AVG. (B) Scanning electron microscopy image of the outer layer. (C) Scanning electron microscopy image of the inner layer of ePTFE graft. 2. Structural design patterns of a woven Dacron graft: (a) plain weave, (b) twill weave, (c) satin weave. 3. Structural design patterns of a knitted Dacron graft: (a) weft knit, (b) warp knit.[28] Reprinted and adapted from ref 28. Copyright 2015 MDPI.

human umbilical vein grafts (CryoVein) and xenografts across species like the bovine jugular graft (Contegra).[10,11] When a small-diameter artificial vascular graft (SDAVG) is used in limb procedures, the patency levels are less ideal than other bypass procedures because of the additional continued stress imposed on the graft by limb flexion. The properties, advantages, and current limitations of the materials in the market are discussed in detail in the following sections.

2. MATERIALS USED IN COMMERCIALIZED VASCULAR GRAFTS

Artificial vascular grafts made from ePTFE and PET have been approved and successfully used as large-diameter (>6 mm) arterial substitutes for more than 40 years. The FDA recently approved PU conduits for commercial use. However, their use in small-diameter applications is still far from ideal. This section discusses the properties of these materials as well as their limitations when used in vascular applications.

2.1. Polytetrafluoroethylene. Expanded polytetrafluoroethylene (Teflon, Gore-tex) grafts have been used as vascular conduits since 1975.[12] The graft is fabricated through heating and mechanical stretching, resulting in a porous structure containing solid nodes interconnected by fine fibrils. The pore size, or fibril length, varies and determines the graft characteristics.[13,14] Its average porosity is described by the internodal distance (IND), usually 30−90 μm.[15] PTFE is used in vascular grafts as it is chemically inert due to the strong fluorine backbone on the carbon chain[16] and is highly electronegative, which minimizes its reaction with blood components.[13] Because of its inertness, no graft failures due to degradation have been reported. In addition, PTFE grafts have moderate stiffness, which increases after implantation due to perivascular reaction.[17]

E-PTFE grafts are preferred for use in small-diameter applications. Despite being the preferred graft for below the knee bypass procedures, its performance is still very poor, with the patency rate reported to be less than 40% after 3 years.[16,18] Functionalizing its surface with heparin has been adopted commercially, but it still offers relatively modest improvements over untreated equivalents.[18,19] Other efforts to improve the hemocompatibility of the PTFE surface to enhance endothelialization and prevent thrombosis have been made by physical or chemically modifying the luminal surface with various coatings, including RGD, elastin,[18] hyaluronan,[16] superhydrophobic and superhydrophilic modification,[20] silk fibroin,[21] endothelial cell seeding,[22] and plasma treatment.[23]

2.2. Polyethylene Terephthalate. Polyethylene terephthalate (Dacron) is another graft that has been available in the market since the 1950s.[12] It is a thermoplastic polymer used as synthetic fibers with a round cross section. These fibers are bundled into multifilament yarns, woven (over-and-under pattern) or knitted (looped fashion) into textile vascular graft fabrics and tubes. Knitted Dacron is impregnated with albumin, collagen, or gelatin to make it more impervious and avoid the need for blood preclotting prior to implantation. In addition, a crimping technique (an undulating surface) is often used to increase its distensibility and kink resistance.[15] PET grafts vary in shape, crimping, fabrication method, and porosity.

Weaving results in narrow spaces for tissue ingrowth, whereas knitting leads to a very porous structure. Of the two structures, surgeons have been reported to prefer the woven

https://doi.org/10.1021/acsomega.2c01740
ACS Omega 2022, 7, 22125−22148

PET, as it is known for its high bursting strength, low permeability to liquids, and minimal tendency to deform under stress.[14] Additional limitations with PET grafts involve progressive graft dilation and mechanical failure. Similar to PTFE grafts, researchers have been working on the long-term patency of PET grafts. In recent work with PET vascular grafts, most research involves using electrospinning[24,25] as the fabrication technique to enhance the topography. To alter the mechanical properties, it has been mixed with elastomeric polymers such as PCL to improve the SDAVGs' compliance.[25] Furthermore, the surface of the PET graft has been modified with bioactive or passivating substances[26,27] to combat thrombus formation and intimal hyperplasia. Figure 1 shows images of the ePTFE and PET grafts.

2.3. Polyurethane. Polyurethanes were adopted as vascular materials based on their elasticity and ease of handling.[14] PUs have been used for various medical applications, including heart valves, dialysis membranes, breast implants, aortic grafts, and bone adhesives. PUs are synthesized by reacting soft (amorphous) segments of polyesters, polyether, or polycarbonates with hard (crystalline) segments of diisocyanates using chain extenders such as diols or diamines. Their properties can be easily enhanced by adjusting the soft or hard segment composition, chain extender, and the molar ratio of individual components.[29] PUs are considered to be biostable; however, some of them eventually degrade in vivo, leading to aneurysms. Polyester-based PU is susceptible to hydrolytic degradation in the body, whereas polyether-based PU is prone to oxidative degradation.[30] Moreover, PU is prone to environmental stress cracking in vivo.

Using a soft polycarbonate segment is a good strategy to develop a polymer that is far more resistant to biodegradation than its predecessors. Polycarbonate-based polyurethane (PCU) is hydrolytically and oxidatively stable.[30] However, its disadvantages include high hydrophobicity and unsatisfactory or nonspecific cell adhesion and proliferation.[15,31]

Another method to overcome these limitations is replacing the hard segment, which is susceptible to degradation, with a siloxane to form polyurethane siloxanes such as polydimethylsiloxane (PDMS).[32] Silicones are biocompatible, biodurable, hydrophobic, have low surface tension, and are chemical and thermally stable. PDMS possesses organic segments derived from PU and inorganic siloxane structures, which combine silicone's chemical stability and PU's elastic nature.[33] Furthermore, siloxane molecules have been reported to reduce platelet and thrombin adsorption. Hence the addition of such groups has been postulated to confer an antithrombogenic effect.[34] Recently, a composite consisting of a polycarbonate segment (PCU) and polyhedral oligomeric silsesquioxane (POSS) emerged. POSS−PCU consists of a PCU polymer backbone that is reacted with POSS nanoparticles, augmenting its mechanical and degradative resistance properties. Silsesquioxanes are silicon-based nanostructures that exist as chain- or ladder-type structures. The polymer is nontoxic and has demonstrated resistance to degradation by plasma proteins and hard and soft segments compared to PCU.[34]

Despite the potential shown by the materials currently being used in vascular grafts, there are still limitations that need to be addressed for their successful application in small-diameter vessels, which has facilitated the shift in focus of research from bioinert to bioactive finally to biomimetic SDAVGs.

3. CHALLENGES IN EXISTING ARTIFICIAL GRAFTS

A human artery comprises three main layers: tunica intima, tunica media, and tunica externa (adventitia).[3] The blood-contacting innermost layer, the intima, comprises a single layer of longitudinally aligned endothelial cells (EC) lining the surface of the lumen, acting as a luminal barrier while providing cellular signaling that prevents thrombosis, infection, and inflammation. These cells adhere to the internal elastic lumina comprising collagen and laminin. Beyond this basement membrane is a media layer composed of circumferentially aligned smooth muscle cells (SMCs) supported by connective tissue (composed of elastic and collagen fibers). Based on signals from nerves within the vessel, these smooth muscle cells will contract or relax, resulting in vasoconstriction or vasodilation. This media is sandwiched between the internal and external elastic lamina, fenestrated elastin layers that interface with the intima and the adventitia, the outermost layer of the arterial wall. The adventitia consists of fibroblasts in a loose extracellular matrix (ECM) mainly composed of collagen. The ECM of native vessels contains a network of multiple proteins in the media and adventitia, which serve distinct mechanical and biochemical purposes. Collagen is the primary component of the ECM, providing tensile strength. Another major component is elastin, which provides elastic recoil to the arterial wall and modulates the proliferation of endothelial cells and SMCs.[11,35−37] Mimicking the structure and function of the artery has been a great challenge in the development of prosthetic grafts, resulting in the short term patency of current commercial grafts. Despite early success in the development of vascular grafts for small vessels, there are still many limitations in the applications of the grafts, including infection, thrombosis, and intimal hyperplasia.[10,38]

An ideal vascular graft should imitate the framework and constitution of native vessels, withstand the hemodynamic in vivo environment, and inhibit nonspecific protein deposition, blood coagulation, and immunological rejection.[39] In addition, it should possess "off-the-shelf" availability in various sizes for emergency care, operative suturability, and simplicity of surgical handling.[15] Because restenosis of the graft for below the knee surgical procedures is mainly a consequence of intimal hyperplasia (IH) at the distal anastomosis and thrombosis. The current strategies to increase the patency of small-diameter vascular grafts focus on matching biomechanical properties and rapid endothelialization.[40,41] Other limitations that have been identified with the current commercial vascular grafts include[6,11] bioincompatibility, leading to thrombosis, embolic events, occlusion, leakage, tearing at the suture line, allergic reactions, aneurysm, and kinking.

3.1. Intimal Hyperplasia. IH is the thickening of the intima, resulting in reduced lumen diameter due to the migration and proliferation of vascular smooth muscle cells (VSMCs) from the media to the intima and deposition of the extracellular matrix.[42,43] IH develops as early as 6 weeks after bypass surgery; its definite cause in vascular grafts is yet to be determined. However, the triggers attributed to its development are endothelial damage during surgery, suture technique, material bioincompatibility, and biomechanical mismatch.[44−46]

3.1.1. Suture Line Stresses. The suture technique used in bypass surgery affects the stress applied to the suture line. Distortions in the native vessel due to the holes formed by the sutures as well as the tension due to their presence cause

https://doi.org/10.1021/acsomega.2c01740
ACS Omega 2022, 7, 22125−22148

Table 1. Compliance Values in Artificial Grafts on the Market and Autologous Grafts

graft name	polymer	wall thickness (μm)	pressure (mmHg)	compliance (%/100 mmHg)	ref
Gore-tex	ePTFE	454 ± 4	50−90	0.0036 ± 0.001	
			80−120	0.0034 ± 0.0004	55
			110−150	0.0033 ± 0.0005	
Zeus, Orangeburg	ePTFE	100	80−120	3.50 ± 1.4	56
SW-ePTFE woven Vascutek Co.	ePTFE	694 ± 14	50−90	0.2	
			80−120	0.6	57
			110−150	0.6	
ePTFE grafts, Impra, UK	ePTFE		30−100	1.2 ± 0.3	58
CPU, CardioTech International, UK	PC		30−100	8.1 ± 0.4	58
	PU				
Silkothane	PCU/SF	335 ± 68	80−120	4.8 ± 1.0	59
Dacron	PET		80−120	1.9	
polyester (woven)			80−120	2.3	28
polyester (knitted)					
uncrimped knitted Dacron graft, Sulzer Vascutek, UK	PET		30−100	1.8 ± 1.2	58
young coronary artery	human		50−90	8.92 ± 7.67	
			80−120	3.39 ± 6.03	60
			110−150	2.69 ± 0.89	
old coronary artery	human		50−90	4.01 ± 2.08	
			80−120	4.06 ± 3.16	60
			110−150	3.42 ± 1.72	
mammary artery	human		50−90	21.05 ± 26.04	
			80−120	5.22 ± 5.13	60
			110−150	1.79 ± 1.96	
			80−120	11.5 ± 3.9	61
radial artery	human		50−90	5.66 ± 2.12	
			80−120	2.05 ± 3.68	60
			110−150	1.06 ± 4.73	
external iliac artery	human		30 to 100	8.0 ± 5.9	58
saphenous vein	human		50−90	2.60 ± 1.72	
		3.46 ± 1.21	80−120	1.77 ± 0.20	60
			110−150	0.67 ± 0.89	
			30 to 100	5.0 ± 6.0	58
				4.39 ± 0.8	62
umbilical artery	human		80−120	5.8 ± 3.1	61
heterograft	bovine			2.6 ± 0.3	63

concentrations of force and increased circumferential tension in the vessel wall adjacent to the anastomosis.[6] A continuous suture line rather than an interrupted line results in a greater concentration of stresses at the suture line. End-to-end anastomosis has also been reported to cause more stress than other techniques, such as the end-to-side. Clips that do not penetrate the intima result in an anastomosis with a less mechanical mismatch.[17]

3.1.2. Endothelial Damage and Material Bioincompatibility. Endothelial cells play an important role in maintaining vascular hemostasis and patency by releasing regulatory molecules including nitric oxide (NO), heparins, plasmin, and tissue plasminogen activator (tPA) to modulate the antithrombogenesis process.[5] Injury to the arterial wall results in exposure of the subintima and media to multiple growth factors, which bind to cell receptors.[6] The injury exposes the ECM, which then attracts platelets and leukocytes from the blood and triggers the process of thrombosis. T-Lymphocytes have also been observed in the intima of injured vessels by secreting tumor necrosis factor-α (TNF-α), which has been proven to induce migration of SMCs[44] due to phenotypic switching from a contractile to a synthetic state.[8,9,47] Thus, damage to the vessel wall decreases the production of growth-inhibiting factors and increases the expression of growth-stimulating factors, shifting the balance to VSMC proliferation.[37,42] Due to the thrombogenicity of the surface of most commercialized synthetic vascular grafts used in small-diameter applications, their presence in the body after bypass surgery triggers the body's immune response system (foreign body response), causing nonspecific protein deposition and provoking thrombogenesis and inflammation.[8] The inflammatory response stimulates the production of matrix metalloproteinases (MMPs) by VSMCs, facilitating the migration and proliferation of VSMCs.[44] MMPs belong to a group of zinc-dependent proteases and cause the breakdown of extracellular matrix proteins such as collagen and elastin, a prerequisite for the migration of VSMCs.[48]

3.1.3. Biomechanical Mismatch. Research has shown that local hemodynamics play a major role in the development and progression of IH.[49] Compliance mismatch between the prosthetic graft and the native vessel has been reported to result in significant hemodynamic disruptions that trigger IH.[50] Compliance can be defined as the change in diameter with pressure change.[51] A study by Post et al.[51] proved the relation between compliant mismatch and the formation of IH by studying the effect of compliance on arterial remodeling in an

https://doi.org/10.1021/acsomega.2c01740
ACS Omega 2022, 7, 22125−22148

ex vivo organ culture model and examining the grafts for identifying early markers of intimal hyperplasia. The arterial wall acts as an elastic reservoir, absorbing energy during systole and releasing it in diastole and introducing a rigid segment, such as a stiff synthetic graft, interferes with this function.[44] This mismatch results in stagnation points, which trap platelets and cause platelet aggregation downstream. The geometric discontinuity across the anastomoses between grafts and native blood vessels creates flow separation and reversal, inducing endothelial injury and endothelial dysfunction.[6]

Endothelial dysfunction reduces the production of tissue plasminogen activator, nitric oxide, and prostacyclin.[52] Furthermore, endothelial dysfunction elevates plasma fibrinogen, thus contributing to prothrombotic activity.[53] In addition, flow reversal and the accompanying wall shear stress (WSS) gradient alter endothelial morphology, disrupt the endothelial barrier function, promote monocyte deposition, induce thrombus formation, and promote gene expression favoring vascular lesion development.[49] In most cases, the response to the flow disruption, the vessel wall attempts to correct it with intimal thickening, ultimately leading to reocclusion.[6,17,49] Such hemodynamic disruptions also transform the shape of endothelium cells from spindle-shaped to round and also affect the expression of some vasoactive molecules. These include nitric oxide synthetase, endothelin, platelet-derived growth factor, transforming growth factor-β1, and some adhesion molecules that can modify endothelial cell function.[42,54] These vasoactive molecules are involved in the formation of IH. WSS, the tangential frictional force acting longitudinally on the vessel wall, imposed by fluid motion on a solid boundary parallel to the fluid direction, regulates the function and composition of blood vessels by affecting the phenotype and integrity of endothelial cells.[9] Neither high nor low WSS is conducive to normal endothelial function. Very high wall shear leads to denudation of endothelial cells, exposure of a thrombogenic surface, and creation of a VMSC proliferative environment,[49] whereas low WSS reduces blood velocity, decreases the proliferation of ECs, and promotes an altered morphology.[44] IH mainly occurs on the arterial floor, heel and toe of the distal anastomosis due to blood flow pattern changes in that region.[46] Other mechanical factors that are thought to stimulate the formation of intimal hyperplasia are suture line stress, which results in distortions in the native vessel. This distortion happens due to the holes formed by the sutures as well as the tension due to their presence, causing concentrations of force and increased circumferential tension in the vessel wall adjacent to the anastomosis.[6] Table 1 shows the compliance values of some of the grafts in the market as well as the compliance values of autologous vessels used in bypass procedures.

4. STRATEGIES TO PREVENT INTIMAL HYPERPLASIA IN VASCULAR GRAFTS

Imitating the natural way an artery functions is an effective strategy to combat IH. Biomimicry in a vascular graft is a challenge due to the complex nature of the artery in terms of both the unique biomechanical properties and supporting tissue regeneration. For both the vascular scaffold used to replace diseased arteries and a permanent artificial prosthesis used in bypass procedures, a long segment (greater than 5 cm) is needed to repair or replace peripheral arteries. Supporting tissue regeneration in vascular scaffolds while maintaining the graft's mechanical integrity is crucial in below the knee procedures, given the length of the graft. The strategies documented in this review consider the duration required for complete tissue regeneration in vascular scaffolds and the mechanical integrity in the permanent vascular prosthesis, hence the need for very slow degrading to biostable polymers. To fabricate vascular grafts that prevent intimal hyperplasia formation for long-term patency, researchers have used various strategies, including passivating the surface to nonspecific protein and platelet adhesion while facilitating rapid re-endothelialization for the blood-contacting lumen. A combination of both elastomeric and mechanically stable polymers to match the viscoelastic properties of the artery is necessary. Furthermore, enhancing or combining fabrication techniques to attain the required biomechanical properties is needed. Figure 2 shows a schematic of an example of a femoropopliteal bypass.

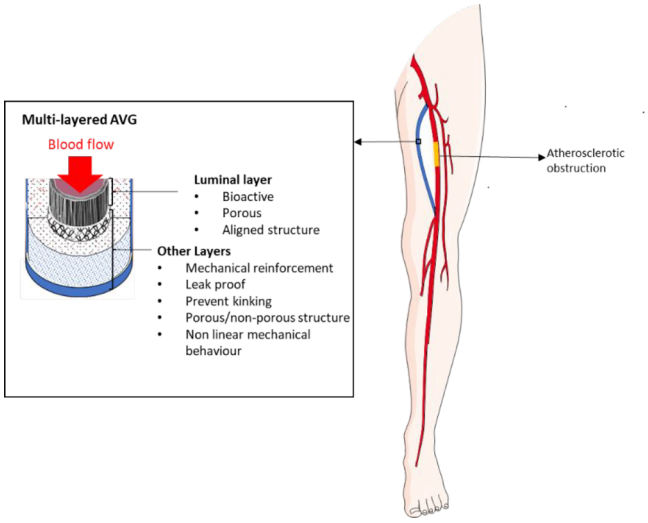

Figure 2. Schematic of femoropopliteal bypass.

4.1. Luminal Layer (Blood-Contacting). *4.1.1. Rapid Endothelialization and Suppression of Nonspecific Protein and Platelet Adhesion.* As mentioned before, the endothelial layer is responsible for anticoagulation and thrombogenesis as well as facilitating the exchange of nutrients and waste. A review by Zhuang et al.[5] provided a fully detailed explanation of the problems experienced in the full re-endothelialization of vascular grafts. In order to promote the endothelialization rate of implanted vascular grafts and to minimize the formation of IH, various strategies have been used, such as providing a superhydrophilic or superhydrophobic surface,[64] the use of natural polymers to provide bioactive binding sites,[65] altering the surface structure, as well as cell seeding.[66] However, some naturally occurring and synthetic polymers already possess the required chemical and biological cues to enhance re-endothelialization and deter nonspecific protein and platelet adhesion. To maximize these cues, some fabrication techniques aid in providing an architecture to support and enhance cell adhesion and migration. This type of architecture provides direction and sufficient porosity, for instance, the use of ridges and grooves as well as a nanofibrous structure.

4.1.2. Bioactive Polymers. Using chemical, biological, and physical cues based on the ECM, researchers are coming up with various ways of enhancing endothelialization and reducing the adhesion of other blood components on developed

https://doi.org/10.1021/acsomega.2c01740
ACS Omega 2022, 7, 22125−22148

vascular grafts. The application of peptide ligands, growth factors, antibodies, magnetic molecules, oligosaccharides, and aptamers have been used for this purpose. Peptide ligands, responsible for binding to receptors on the corresponding cell, have been produced from ECM proteins such as collagen, fibronectin, vitronectin, and laminin. The most common peptide ligands that have been researched for application in vascular grafts include RGD, YIGSR (laminin-derived), REDV (fibronectin-derived), and CAG (collagen-derived).[67] Natural polymers such as collagen, elastin, silk fibroin, gelatin, hyaluronan, and fibrin can provide enough cellular ligands for enhanced cell adhesion in vascular graft fabrication. However, these polymers possess nonspecific binding sites for other blood cells like platelets, white cells, and SMCs, which may induce thrombogenesis and IH.[5] ECM-derived polymers like collagen, elastin, and fibrin contain the Arg-Gly-Asp (RGD) cell recognition signal that allows the cell-membrane-bound integrins to bind.[68] However, nonselective peptides might mediate the adhesion of different cells and result in competition between ECs and other cells, hindering the future formation of the endothelium.[69] The peptides YIGSR and REDV contain more specific binding sites than RGD; these are used to recruit circulating endothelial progenitor cells and engage adjacent adult cells for endothelialization and extracellular matrix regeneration.[40,70] The $\alpha 4\beta 1$ integrin, which is abundant on ECs and scarce on SMCs, can specifically bind to REDV, and the 67 kDa laminin-binding protein highly expressed on the surface of ECs easily binds to YIGSR.[65] Therefore, critical preservation of the nonthrombogenic and endothelialized surface is crucial, i.e., active components should be stable long-term.[71] CAG has also been utilized due to selectively promoting EC adhesion and exhibiting a low adhesive tendency toward SMCs preventing the formation of IH.[31]

Isolated growth factors responsible for regulating angiogenesis and modulation of endothelial cell function can also be used to stimulate EC proliferation and migration. Such growth factors include vascular endothelial growth factor (VEGF), fibroblast growth factor-2 (FGF-2), transforming growth factor-beta (TGF-β), platelet-derived growth factor (PDGF), hepatocyte growth factor (HGF), and recombinant human tropoelastin (rhTE).[72] Review papers by Gomes et al.[73] and Goh et al.[74] have thoroughly documented the different types of peptides and growth factors that have been used to promote rapid endothelialization in cardiovascular applications. The following section gives detailed descriptions of natural biomaterials and their effect on IH.

4.1.2.1. Natural Polymers. Collagen and elastin are responsible for the viscoelastic behavior of blood vessels, together with the aid of SMCs through vasodilation and vasoconstriction. Collagen was initially studied for use in vascular grafts because of its naturally occurring presence in the human arteries. Collagen, a component of natural ECM, possesses excellent biocompatibility, provides biological signals to adherent cells, and promotes tissue regeneration.[75] The final properties of collagen are determined by the isolation and purification processes, type of cross-linking, and fabrication technique. The most prevailing and investigated collagens are types I and II, with type I being the most prominent.[75−77] Sources of collagen are calf bovine, porcine, and aquatic life. A study by Lambert et al.[78] investigated the immunological response of vascular grafts coated with collagen from aquatic and bovine sources. Their results indicated that the collagen from freshwater fish elicited lower immunological reactivity to bovine collagen in an animal model. As collagen is naturally a thrombogenic material, using it as the luminal layer in vascular grafts triggers platelet adhesion, activation, and aggregation, which is one step towards healing, however, the graft occluding as well.[79,80] This was shown in a study by Kumar et al.,[81] where they fabricated a vascular conduit comprising collagen fiber networks and elastin-like protein polymers. They conducted platelet adhesion and activation on various substrates: glass, ePTFE, collagen, elastin, and their developed graft. They found that glass had the largest number of adherent platelets, followed by collagen, ePTFE, elastin protein polymer, and protein composite conduits' luminal surface. Different strategies have been used to reduce the thrombogenicity of collagen, including mixing with elastin, as shown in the same previously mentioned investigation by Kumar et al.,[81] in which a combination of elastin and collagen showed promising results with patency results after 14 days in vivo with no thrombus or visible intimal hyperplasia. In another study by Koens et al.,[82] a three-layered porous graft (elastin−collagen−collagen) was fabricated using highly freeze-dried, purified type I collagen fibrils and elastin fibers. Comparing their graft with a heparin-coated ePTFE commercial graft, in vivo results after 4 weeks showed that the collagen−elastin grafts were fully occluded with layered thrombi while only 25% of the ePTFE graft was found to be occluded. Calcification was also observed in the elastin layer.[82]

Elastin provides the necessary elasticity to support the unique viscoelastic mechanical behavior of blood vessel walls. The presence of elastin in the arteries aids in inhibiting smooth muscle cell migration and proliferation and enhances endothelial cell adhesion and proliferation.[83] Incorporating elastin into vascular implants has been shown to reduce thrombogenicity and platelet adhesion and activation, translating to improved patency in vivo. Incorporating elastin in collagen has been shown to improve elasticity and reduce the thrombogenicity of collagen. A study by Wong et al.[77] analyzed the cellular response of PU/elastin, PU/collagen, as well as PU/collagen/elastin. Seven days of culture of SMCs demonstrated that collagen-blended PU scaffolds had the highest cell number, increasing 2.83-fold over PU scaffolds. PU combined with collagen and elastin increased cell proliferation by 2.23, and elastin did not promote SMC proliferation compared to unmodified PU. Wise et al.[83] electrospun a graft with PCL and recombinant human tropoelastin, the soluble precursor of elastin. Platelet adhesion tests confirmed that the elastin-coated conduits reduce platelet attachment compared to bovine serum albumin and collagen-coated surfaces. In the same study, when platelet attachment was compared on PCL, PCL/elastin, and PTFE graft, platelet adhesion was substantially reduced on the PCL/elastin compared to bare PCL and the PTFE graft.

Gelatin is denatured collagen, soluble in water, and proposed here as a low-cost alternative to soluble collagen.[84] Gelatin has relatively low antigenicity compared to collagen, and it possesses cell surface binding ligands RGD, which are favorable for cell adhesion.[85] Incorporating gelatin in potential vascular grafts or scaffolds increases the cell growth rate by providing the required hydrophilicity and is widely used with various materials such as PCL,[86] PLLA,[87] PLA, PU,[88] PLGA,[89] and PGA.[90] Gelatin also reduces platelet and protein adhesion, as shown by Johnson et al.,[91] on coaxially electrospun PCL−gelatin vascular scaffolds. The number of adhered platelets on

https://doi.org/10.1021/acsomega.2c01740
ACS Omega 2022, 7, 22125−22148

coaxial PCL/gelatin fibers decreased by 75% compared to PCL fibers. This was further proven by an in vivo study with the same group. It was shown that the explanted multilayered coaxially electrospun grafts revealed no blood clots or platelet adhesion with no unfavorable systemic inflammation or thrombogenic reactions after 3 months in vivo.[91] To further improve the immunogenic properties of gelatin, other molecules such as heparin,[92] bivalirudin,[93] functionalizing with methacrylic anhydride,[94] and drug loading, for instance, with telmisartan,[95] have been used. The most common fabrication technique using gelatin for the blood-contacting layer is mixing it with another polymer,[95,96] as a hydrogel,[97] and forming a core−sheath structure (gelatin as the sheath and a variety of polymers as the core).[88,91,94]

Hyaluronan/hyaluronic acid (HA) is a naturally occurring polysaccharide and a major extracellular matrix component.[98,99] It is a hydrophilic, non-adhesive (low molecular weight HA), an antithrombogenic and non-immunogenic biocompatible natural polymer. HA rapidly biodegrades, and depending on the molecular weight, it is both mitogenic for ECs and bacteriostatic.[100] It can bind to the cell surface receptor CD44 to modulate cell differentiation, migration, and angiogenesis without eliciting any foreign-body response, making it an intriguing material for vascular application.[101] High molecular weight HA inhibits EC proliferation, whereas low molecular weight HA oligosaccharides (0.75−10 kDa) stimulate EC proliferation and migration. HA has also been found to inhibit fibroblast proliferation, which is another action that may assist in the prevention of graft occlusion.[100] In addition, HA has been noted to promote vascular smooth muscle regeneration, which might not prevent IH in the intima layer unless targeted for a specific goal layer, such as the media layer.[102] Hyaluronan oligomers are biofactors that have been shown to improve elastogenesis in adult cells, another positive effect in the fight against IH when developing AVGs.[103] Several conducted studies have proved the nonfouling nature of HA.[104,105] An esterified form of HA known as Hyaff-1, which does not elicit an inflammatory response and degrades into gel formation as found in the ECM, thereby suppressing a macrophage-mediated response resulting from polymer degradation, has also been reported.[98,104] Despite the increases in EC regeneration on the lumen of a developed graft, an in vivo study using esterified HA by Pandis et al.[104] showed IH formation after 30 days of implantation due to a geometrical mismatch between the vena cava and prosthesis. IH formation, however, decreased with increasing time points. HA can be used in hydrogel form[106] and electrospun with PU,[100] collagen,[105] and various other methods for the luminal layer.

Other ECM proteins and components that have been used to enhance cell adhesion, proliferation, migration, and differentiation are fibrin, fibrinogen, laminin, and fibronectin.[99,107] These proteins are derived from plasma proteins in blood components. They are nontoxic, biocompatible, and do not trigger an obvious immune response.[108] Fibrin and fibrinogen are involved in blood clotting during the coagulation cascade[109] and can be obtained from salmon, human, or bovine sources. Fibrinogen is isolated from blood plasma and cleaved with thrombin to form fibrin.[110] Because of the rapid degradation rates of fibrin, it is generally combined with laminin, collagen, or HA to slow down the degradation process.[98] Laminin is a glycoprotein of the ECM that is generally found in the basement membrane[111] and contains binding integrins ($\alpha_7\beta_1$, $\alpha_6\beta_1$, $\alpha_3\beta_1$), which mediate interactions between ECs and vascular scaffolds.[99] Fibronectin, another ECM protein, interacts with cells via the integrins $\alpha_5\beta_1$ or $\alpha_v\beta_3$, which makes it a suitable bioactive protein for endothelialization, and it is also known to play a pivotal role in wound healing.[112] These proteins may be used as coatings in hydrogel form,[13,99,113] or otherwise combined with synthetic polymers such as PLGA,[114] PCL,[109] and PU for electrospinning[112] and combined with other combinations of natural polymers such as silk fibroin[111] and fucoidan.[115] In comprehensive detail, Filová et al.[107] investigated the adhesion and differentiation of ECs on ECM-derived proteins: collagen type 1, laminin, fibronectin, and fibrin. Their results from coated polystyrene with all four ECM proteins showed that seeded ECs reached the same densities on all surfaces after 24 h. An increase in EC proliferation was visible only after 48 h only for collagen 1 and fibronectin coatings.

Although not ECM-derived, silk is another naturally occurring polymer with bioactive sites. Silk fibers are produced from a wide variety of spiders and Lepidoptera worms; however, most of the fibers used are obtained from the cocoons of the *Bombyx mori* silkworm.[116] Silk has been used in a wide array of biomedical applications such as suturing and ligatures, skin repair, retina replacement, drug delivery applications, tissue engineering, or implantable devices.[41,117] The two active components of silk are fibroin and sericin. Silk fibroin (SF) is the core filament of silk consisting of highly organized β-sheet crystal and semicrystalline regions responsible for silk's elasticity.

In contrast, sericin is an antigenic gum-like protein surrounding the fibers.[118,119] The advantages of silk fibroin as a biomaterial are good cytocompatibility, tailorable biodegradability, suitable mechanical properties, and minimal inflammatory reactions.[27] Most studies with SF as a blood-contacting layer in vascular grafts mainly use it as a porous sponge inner layer or a coating on braided SF.

A common method of fabricating the luminal layer with SF is gel spinning, which mimics spinning silk protein in silkworms. The diverse winding and postwinding processing options enable the construction of the final material to be controlled, and fiber diameters smaller than a few microns can be produced.[116] The gel-spinning process relies on high concentration (i.e., >20% w/v) silk solutions. This helps in maintaining the shape of the artificial grafts when extruded due to increased crystallinity of the viscous solution.[120] A couple of studies have shown that the use of SF in the luminal layer aids in preventing the formation of IH in vascular grafts. For instance, in a study by Tanaka et al.,[27] they coated a PET braided graft with a silk fibroin sponge and compared it to a gelatin-coated graft. Three months after in vivo studies, tissue remodeling was high in both grafts; however, signs of thrombus formation and intimal hyperplasia were observed in the gelatin-coated PET graft shown by the higher percentage of macrophages and not in the SF-coated PET graft. In another study by the same group,[121] a 0.9 small-diameter braided SF vessel was coated with an SF sponge and implanted into mouse carotid arteries. Despite showing a high mean endothelial coverage, the patency rate was not high enough (13.3%) after 6 months in vivo, and thrombosis was sighted as the cause of stenosis.[121] In another study by Fukayama et al.,[119] an SF coating in various concentrations was applied to a double-raschel knitted small-sized vessel. The results showed that a concentration of 2.5 wt % was the optimal concentration after in vivo implantation in terms of enhanced tissue infiltration

https://doi.org/10.1021/acsomega.2c01740
ACS Omega 2022, 7, 22125−22148

and preventing IH. However, excessive vascular intima by smooth muscle cells was observed in 5.0 and 7.5% SF coating and was responsible for stenosis after 3 months. In order to further improve the biocompatibility of SF, anticoagulants such as heparin or sulfonated SF may be utilized to combat the minimal immune adverse response that SF may elicit. Zhang et al.[21] modified a 4 mm commercial ePTFE graft with sulfonated SF. After 3 months in vivo, endothelial cell adhesion and proliferation on a sulfonated SF-coated graft (84%) was much better than that on the bare ePTFE (11%), and hardly any thrombosis was observed in the SF-modified grafts. These results indicated that the SF-modified experimental grafts might have good long-term patency due to the anticoagulant function of the SF film and rapid formation of the endothelium, which can prevent blood vessel thrombosis or intima hyperplasia. Liu et al.[122] fabricated a SF bilayered graft from a braided inner layer containing heparin and a highly porous lyophilized outer layer. Platelet adhesion was reduced significantly with increasing heparin concentrations, and blood compatibility was effectively enhanced with the introduction of heparin.

Chitosan is a natural hydrophilic polymer (polysaccharide) with sufficient mechanical strength in its wet state, with the presence of reactive groups and antibacterial properties. It is a natural amino polysaccharide capable of absorbing large amounts of water, second to cellulose and chitosan hydrogels. Like other polysaccharide-based hydrogels, it partly mimics the glycosaminoglycan components of the ECM. The biodegradation of chitosan can be optimized by changing their degree of acetylation.[123] However, one disadvantage of chitosan is its poor hemocompatibility because the cationic profile causes the unnecessary adhesion of negatively charged platelets, limiting its application in vascular tissue engineering.[124] Aussel et al.[123] investigated the potential use of chitosan in vascular grafts, and they concluded that endothelial progenitor cell (EPC) viability and migration were greater on the plastic control than on chitosan hydrogels. However, with in vitro hemocompatibility tests, the results were more promising, with the chitosan hydrogels being nonthrombogenic and "nonactivating". This was further supported by the short-term in vivo studies, which showed that the chitosan hydrogels did not induce chronic inflammation.[123]

Another naturally occurring polysaccharide is alginate, which is composed of β-D-mannuronate and α-L-guluronate. Divalents such as Ca^{2+}, Sr^{2+}, and Ba^{2+} render alginates insoluble in water. In the presence of these divalents, the alginates form chains, subsequently leading to gelation. Due to their biocompatibility and nontoxicity, alginate gels have been used in biomedical applications such as dental impressions, drug delivery devices, and as immobilization matrices for cells.[125]

Apart from natural polymers like the ECM-derived polymers, which contain bioactive molecules for the promotion of rapid cell adhesion, proliferation, migration, and differentiation, other compounds may be used in association with these natural polymers to enhance re-endothelialization of an AVG and deter the nonspecific protein and platelet adhesion. These compounds include anticoagulants, drugs, and antifouling materials.

4.1.2.2. Anticoagulants. Anticoagulant modifiers, such as zwitterionic polymers, hydrophilic PEG, growth factors, and heparin, have been widely investigated in blood-contacting materials. It is critically important for vascular graft surfaces to maintain long-term antithrombotic performance until complete endothelialization is done.[126] Activated platelets and thrombin promote NIH by their mitogenic effects on SMCs, so techniques that reduce graft thrombin activity may have more far-reaching effects on graft patency.[127] Heparin is a glycosaminoglycan (GAG) composed of alternating glucosamine and uronic acid sugars and is extensively sulfated to confer a high degree of negative charge. Heparin is stored in mast cells and secreted by endothelial cells, thereby forming part of the blood vessel extracellular matrix. Heparin has both anticoagulant properties and vascular smooth muscle cell antiproliferative properties, and it shows these properties both in vivo and in vitro.[124,128] It has also been extensively applied for thromboembolic disease treatment, as well as cardiovascular and peripheral vascular surgery.[129] The application of heparin in vascular grafts is widespread. However, the major setback is its controlled, long-term release and hemorrhagic effect. Methods used to impart heparin into vascular grafts include physical conjugation methods such as gas plasma, straight mixing with sulfated biopolymers, and coaxial electrospinning. Chemical conjugation methods contain covalent and ionic bonding.[130] Zhu et al.[64] covalently bonded heparin with PEG to poly(ester urethane)urea (PEUU) and resulted in no thrombosis within the lumen after 30 days in vivo.

The PEG and heparin enhanced the anticoagulant capacity, conferred rapid endothelization by increasing the surface wettability, and limited intimal hyperplasia. In a study done by Yao et al.[124] The functional groups in chitosan were utilized to immobilize (ionic bonding) heparin into PCL electrospun grafts, resulting in the sustained release of heparin within a period of more than 1 month. This was further demonstrated by freedom from thrombus, better endothelialization, and patency for the heparin-functionalized PCL/CS grafts compared to the control group after 1 month in vivo. In another study, Wang et al.[131] incorporated heparin by coaxially spinning it into poly(L-lactide-*co*-ε-caprolactone) (P[LLA-CL]) nanofibers. This method allowed the continued release of heparin for 12 weeks. There is a specific affinity between heparin and angiogenic growth factors, and heparin has the capability to increase the stability against thermal denaturation and enzymatic digestion in physiological conditions of polypeptides. Based on this notion, some researchers combine polypeptides (such as QK, RGD, REDV, and YIGSR) and growth factors (VEGF) with heparin and impart them into different polymers. This further promotes rapid endothelialization together with the anticoagulative and antiproliferative properties of heparin.[125,131,132]

Nitric oxide (NO) is responsible for modulating the activation and adhesion of leukocytes. It possesses antithrombogenic properties and provides antiproliferative and migration inhibitory effects on smooth muscle cells which maintains the vascular smooth muscle in a nonproliferative state, preventing adverse vascular remodeling. Moreover, it stimulates EC proliferation and provides anti-inflammatory and antiatherogenic effects by the inhibition of apoptosis.[133] Strategies of incorporating NO in vascular grafts include incorporating known NO donors (S-nitrosothiols (RSNOs), S-nitrosoalbumin (AlbSNO), S-nitrosoglutathione (GSNO), S-nitrosocysteine (CysSNO)), where some copper- or selenium-containing species can accelerate the decomposition and release of NO.[69] Another method is directly designing NO-releasing and NO-generating polymeric materials.[134] The drawbacks of NO

https://doi.org/10.1021/acsomega.2c01740
ACS Omega 2022, 7, 22125−22148

Table 2. Luminal Natural Polymers and Their Performance Against IH

luminal natural polymer	fabrication structure	endothelial cells, smooth muscle cells	compliance, intimal hyperplasia, and patency	ref
gelatin	co-electrospinning with TPU	HUVECs formed a monolayer that almost reached confluence similar to physiological morphology of endothelial cells, with a cobblestone-like arrangement after 6 days. Cells on TPU only were unable to undergo appropriate spreading and proliferation and a rounded morphology.		146
	core−shell structure electrospinning PCL-gelatin PLA-gelatin PU-gelatin	The highest human pulmonary artery EC growth rate reached confluence on PCL-gelatin. With human pulmonary artery SMCs, the highest cell growth rate was on PCL-gelatin.	PCL-gelatin 29.7%/100 mmHg, PLA-gelatin 27.7%/100 mmHg, PU-gelatin 7.9%, umbilical vein ∼3.7%/100 mmHg	88
	electrospinning PCL-gelatin-heparin	At 2 weeks PCL and PCL-gelatin groups showed a thick layer of cells that might have been ECs or platelets. PCL-gelatin-heparin grafts had a thin cell layer similar to that of the native endothelium. After 4 weeks, the endothelial cell layer of the PCL group was discontinuous in comparison with the regenerated endothelium of the PCL-gelatin-heparin. After 2 weeks, the coverage thickness of SMCs in PCL and PCL-gelatin grafts was slightly higher than that of PCL-gelatin-heparin grafts and after 4 weeks growth in PCL-gelatin-heparin was no longer evident.	After 2 and 4 weeks, luminal surfaces of PCL and PCL-gelatin-heparin grafts were smooth at both time points, whereas macroscopic thrombus had occurred within the lumen surface of PCL-gelatin graft implants at week 4.	147
	electrospinning and coating	In vitro rat aortic EC number on PGH grafts was much higher than those of PCL grafts and PH grafts at 48 and 72 h, and rat aortic SMC number on PGH grafts was higher than that on PH grafts at 24 h, but at 48 and 72 h, the number on PCL was much higher than PH and PGH grafts.	Compliance of PGH graft was 7.52 ± 0.93%/100 mmHg and for the PH graft was 9.48 ± 0.93% /100 mmHg	148
	PCL-gelatin-heparin (PGH) PCL-heparin (PH)	In vivo, flat polygonal ECs were found on the PGH grafts after 1 week, with no ECs on the PH graft. After 4 weeks, PGH grafts were fully covered by a continuous layer of ECs, and a smooth endothelium can be observed. ECs covered most parts of the PH grafts, but the endothelium was rough and discontinuous.	No thrombus observed on the internal surface of PH and PGH grafts. PH and PGH grafts were patent, and no significant stenosis was found.	
	electrospinning and hydrogel PU-PEG collagen-mimetic (Scl2-1 and Scl2-2) protein hydrogel, PU-PEG collagen hydrogel	The average bovine aortic EC spreading on PEG-Scl2-2 hydrogels was lower than that on the PEG-collagen controls.	The levels of platelet adhesion on the PEG, PEG-Scl2-1, and PEG-Scl2-2 hydrogels were statistically similar and were each significantly lower than the values for the TCPS and collagen-coated TCPS positive controls. In a pulsatile bioreactor, PEG, PEG-Scl2-1, and PEG-Scl2-2 hydrogels remained patent during the testing time, while the ePTFE (GORE-TEX) vascular graft occluded due to thrombosis within 1 h. Compliance of was 2.7 ± 0.3%/100 mmHg.	149
collagen elastin	electrospinning	In vivo at 14 days, staining of the luminal surface was positive for collagen, mononuclear cells, entrapped red blood cells, and vWF+ cells, suggestive of an endothelial-cell-containing neointima.	Glass had the largest number of adherent platelets ($2.42 \pm 0.10 \times 10^5$ platelets mm^{-2}), followed by collagen ($2.04 \pm 0.09 \times 10^5$ platelets mm^{-2}), ePTFE ($1.62 \pm 0.05 \times 10^5$ platelets mm^{-2}), elastin protein polymer ($6.62 \pm 0.36 \times 10^4$ platelets mm^{-2}), and the luminal surface of protein composite conduits ($6.78 \pm 0.05 \times 10^5$ platelets mm^{-2}).	81
	collagen, elastin		In vivo, at 14 days, grafts appeared patent with a minimal adhesive response to the abluminal surface. Visual observation of graft luminal surface showed no thrombus or visible intimal hyperplasia.	
	electrospinning and knitting collagen knitted (Col-K) collagen knitted and electrospun (Col-KE) control PLA knitted (PLA-K)	More human umbilical vein ECs were spindle-shaped and well-attached to the collagen substrates compared to those on the PLA substrate. The Col-K scaffolds showed significantly superior initial cell attachment and overall cell growth compared to the Col-KE and PLA-K grafts.	Between 80 and 120 mmHg, Col-K had a compliance of 2.81 ± 0.28%/100 mmHg, and Col-KE had 3.06 ± 0.96%/100 mmHg. The PLA grafts (PLA-K) showed significantly higher compliance of 5.42 ± 0.17%/100 mmHg, which was similar to that of a human artery (4.7−17.0%/100 mmHg).	80
	electrospinning PCL/elastin freeze-drying	Human umbilical vein EC attachment and proliferation was compared to BSA, fibronectin and uncoated tissue culture plastic (TCP). Cell attachment to elastin was greater than BSA at all time points and not significantly different to fibronectin but was higher than on BSA and TCP. A substantial covering of HUVECs on elastin and PCL/elastin scaffolds was observed on day 1, increasing out to day 3. HUVECs attached to and spread on PCL, PCL/elastin and elastin scaffold surfaces by day 3.	The elastin coating reduced platelet attachment compared to BSA by 53 ± 1.9% and collagen by 61 ± 7.1 %. Platelet attachment to elastin scaffolds was strikingly reduced by 88 ± 1.6% compared to ePTFE ($P < 0.001$), and importantly by 80 ± 8.4% compared to PCL alone Results showed that both the developed graft (elastin/collagen) and the control (ePTFE) were patent 1 week after surgery. However, 4 weeks post-implantation, all four of the elastin/collagen grafts and	83 82

https://doi.org/10.1021/acsomega.2c01740
ACS Omega 2022, 7, 22125−22148

Table 2. continued

luminal natural polymer	fabrication structure	endothelial cells, smooth muscle cells	compliance, intimal hyperplasia, and patency	ref
	lumina layer-elastin/outer collagen		only one of the ePTFE were occluded. Fibrin infiltrated the surrounding tissue in both the natural and synthetic graft and in the developed graft. Elastin fibers in the luminal layer were dislodged.	
	electrospinning and plasma coating PCL-HA	Immobilization of HA increased the number of adherent mesenchymal stem cells (MMSCs) cells on the surface by more than 65% compared to the surface of the untreated sample (PCL).		150
hyaluronic acid	film PU/polyethylenimine (PEI)-HA (PPHA) PU/PEI-heparin (PPH) PU/PEI−PEG (PPP)	At 5 h post-seeding, cells on all surfaces possessed a highly rounded morphology of bovine aortic ECs. At 5 days, a significant increase in cell number at was achieved on HA and heparin conjugated grafts. Only HA conjugated grafts exhibited a cobblestone pattern typical of ECs and reached confluency by day 5, with more cells adhered than any other condition followed by the PPH grafts.	Only HA-grafted surfaces permitted significantly less protein adsorption than that found on the unmodified PU-PEI control.	151
	electrospinning PU-HA	At 5 h post-seeding, similar numbers of bovine aortic ECs had adhered to both the PU and PU-HA grafts. At day 5, a significant increase in EC number was achieved across PU-HA grafts. However, PU alone had the highest number of ECs.	There was a 50−70% reduction in protein adsorption with PU-HA compared to that with unmodified PU. Incorporation of HA into the PU backbone resulted in significantly decreased platelet adhesion relative to the PU.	152
	electrospinning and coating	Combining collagen IV and laminin together resulted in the highest number of adhered HUVECs after 6 hrs and the highest proliferation rate after 6 days of culture. There was no significant different between the collagen and laminin coated membranes however cell adhesion and proliferation were higher compared to just PCL fibers.	Collagen IV and laminin immobilization had limited influences on BSA adsorption. The surface modified PCL before conjugating with collagen or laminin had the largest platelet adhesion value and showed a dendritic morphology with many extruding filopodia showing a potential to recruit other platelets. On the laminin and collagen modified nanofibers numbers of adhered platelets were significantly lower with some platelets showing a round shape with less filopodia.	153
	PCL-collagen/laminin	Biomolecule immobilization also resulted in increased NO and PGI2 release capability from the HUVECs and this was significantly higher in the laminin coated and laminin and collagen combination fibers than collagen only coated samples.		
	electrospinning PCL/fibrin	Endothelialization coverage value of PCL/fibrin grafts were higher than that of PCL grafts at 1, 3, and 9 months. At 9 months in vivo, compared with PCL grafts, PCL/fibrin grafts showed more cobblestone-like cells covering the surface, slightly less than the native artery. HE staining results showed that PCL grafts showed fewer SMCs and thinner graft wall. The wall thickness and cell number of the PCL/fibrin grafts were close to those of native artery. Results of immunofluorescence experiments showed that the α-SMA expression quantity in PCL/fibrin vascular grafts group was similar to native artery group.	After 9 months in vivo, the luminal surface of the samples was very smooth and clean, and no thrombosis and platelet aggregation were found. However, PCL grafts had significantly more calcification than PCL/fibrin grafts located near the lumen. At 1 month, macrophages oriented with microfibers of PCL/fibrin grafts were observed, and there were many CD68 positive markers. However, as the transplantation time prolonged, the CD68+ macrophages gradually decreased, and by 9 months, their number was close to the native arteries.	154
	electrospinning PCL/fibrinogen	From the hUASMCs seeded, the native umbilical cord artery exhibited organized ECM cells and expressed both α-SMA and calponin, highlighting a functional contractile apparatus. However, the PCL/fibrinogen scaffolds developed a collagenous ECM. There was a limited expression of α-SMA and no positive calponin expression was detected. After 4 weeks in culture, the cells in the PCL only scaffold revealed no distinct organization or orientation, and cellular infiltration was highly heterogeneous. With the PCL/fibrinogen graft, DAPI staining of scaffold cross sections revealed excellent cellularization across the entire thickness of the graft wall with a a circumferential orientation.	After 4 weeks in culture, the appearance and handling properties of the composite scaffold were tissue-like, with smooth union of the layered sheets and excellent patency	155
	bacterial nanocellulose (BNC) with human albumin, fibronectin, and heparin−chitosan coating	In static conditions, for vascular ECs, only fibronectin-coated patches showed multiple large and partially coherent colonized areas but also nonpopulated spots and areas. All other coatings only showed smaller cell islets or singular cells. For endothelial progenitor cells, densely populated areas of EPCs were found for all coatings and also uncoated BNC patches after seeding the cells under static conditions. Under dynamic conditions, the most confluent coverage and highest density was in the fibronectin group, partially confluent areas of VECs were found for the albumin group, while the uncoated group showed a lower density of VECs. The heparin group showed only scattered signals at much lower density. For EPCs, there was very high overage for the fibronectin group. The heparin group was also colonized, but at lower cell densities. The albumin and uncoated groups remained mostly unpopulated, and only scattered cells were found.		156

https://doi.org/10.1021/acsomega.2c01740
ACS Omega 2022, 7, 22125−22148

Table 2. continued

luminal natural polymer	fabrication structure	endothelial cells, smooth muscle cells	compliance, intimal hyperplasia, and patency	ref
	electrospinning PCL, PCL-PEGME (polyethylene glycol methyl ether), and PCL-chitosan	Using RBSMCs, PCL-PEGME, and PCL-chitosan membranes showed similar proliferation rates at 7 days. Different types of SMC markers were highly expressed in RBMSCs cultured on PCL-chitosan electrospun mats than on PCL-PEGME mats.		157
	electrospinning/hydrogel layer	On day 1, all the samples showed the same proliferation intensity. With time, the least cell adhesion and proliferation was observed on the TPU only grafts. As heparin increased the wettability of the grafts, it promoted better adherence. When SF was added, these samples showed enhanced cell viability and attachment; however, with time (1 week), there was a decreased proliferation rate. The combination of SF and heparin resulted in the highest HUVECs growth and proliferation.	With platelet adhesion, the inclusion of heparin into the samples significantly reduced the number of adhered platelets on the surface. Both the TPU only and TPU/SF samples showed an increased amount of platelet adhesion to the extend forming aggregates on the surfaces of the samples.	158
chitosan	TPU-heparin/SF (core/shell structure)-inner layer, chitosan/gelatin-hydrogel (C/G) outer layer	For the outer layer, using SMCs, the 1/1 and 3/1 hydrogel ratios showed almost the same cell growth compared with the blank sample at 1, 3, and 7 days after cell seeding. Sample 2/1 had the least cell adhesion and proliferation, even compared to the control cell with no bioactive polymer.		
	electrospinning PCL/chitosan nanoparticles	Results with human skin fibroblast cells showed that the electrospun PU/chitosan membranes showed enhanced cell attachment and proliferation than the pristine PU membrane. The cell attachment and proliferation percent of pure PU was observed to be 141.9 ± 2.264 and for PU/chitosan nanofibers electrospun at ratio 8:2 (v/v) and 7:3 (v/v) were found to be 181.8 ± 2.611 and 180.8 ± 3.846, respectively.		159
	electrospinning PCL/chitosan	Vascular remodeling was found to still be occurring at the time of explantation, in the neointima. A cellular monolayer stained positively for vWF, indicating endothelial cell layer formation. Some mature and functional smooth muscle cells were detected in the media of the developed graft. Both types of cells were mature and well-organized, which reflected the native carotid artery in area, distribution, and density.	Results showed that after 6 months in vivo, the compliance of the developed graft decreased significantly (from 14.04 ± 1.50 to 6.58 ± 1.76%). The patency rate of the developed grafts was found to be ∼66% (4 out 6 grafts). The decrease in compliance was attributed to an increased presence of collagen in the developed graft. The luminal surfaces of patent grafts displayed no evidence of microthrombosis. The TEVG's wall thickness was however significantly higher than the native carotid artery, resulting from a significant macrophage infiltration into the scaffold.	160
	knitted and sponge	After implanting (in beagles), mild bleeding was observed in the grafts and anastomotic sites. The grafts adhered to the surrounding muscles by thin fibrous tissue. After 1 year in vivo, a layered structure mainly composed of smooth muscle cells, elastic fibers, and collagen fibers was identified.	Occlusion due to thrombus formation was observed 4 weeks post-implantation in 1 out of 6 grafts. In the remaining 5 grafts, there was also no intimal hyperplasia or aneurysms at 3 months, 5 months, and 1 year. Inflammatory cells, such as neutrophils, lymphocytes, and macrophages, were concentrated around the graft but could not be found around the base of the graft or in the lumen at 3 months post-implantation and these decreased with increasing time points.	161
silk fibroin	electrospinning inner and outer layer, braiding-middle layer	Endothelial cells, smooth muscle cells, and adventitial fibroblasts were used for the cell study, and after 3 h of cell seeding, all cell types covered approximately 61 ± 5% of the surface. The polystyrene control had 2.1× less cells than on the SF surfaces. After 20 days, the fibroblast cells seeded onto SF graft increased their number 4-fold, endothelial cells 3-fold, and SMCs 6.5-fold. Contrary to the theory where proliferation is greater on natural bioactive polymers, the polystyrene surface had a 7.5× increase in fibroblast cells, 5× increase in endothelial cells and a 7× increase in SMCs.	To assess the patency of the grafts, ultrasound and angiographic analysis were used at days 13 and 24 post-implantation. The results showed patent grafts with no signs of aneurysm, dilation, dissection, blood collection or signs of infection. The graft implanted in the sheep showed no stenosis, whereas in the minipig, a slight stenosis near the proximal anastomosis was identified. A thin layer of soft tissue was found in the external surface of the graft explanted from the sheep, however that from the minipig had a thicker layer. Signs of an ongoing foreign body response in the stenosis of the graft explanted from the minipig were identified by the presence of collagen fibers, fibroblasts, macrophages, and multinucleated giant cells together with a lesser number of lymphocytes, plasma cells, and neutrophils filling the voids of the middle layer.	162

https://doi.org/10.1021/acsomega.2c01740
ACS Omega 2022, 7, 22125−22148

donors are limited storage, burst release, and toxicity caused by leakage, and thus, long-term efficiency and graft patency could not be guaranteed. In situ catalytic NO generation is a better approach to incorporating NO in vascular grafts. Enayati et al.[134] used an NO donor, S-nitroso human serum albumin, in a PCL electrospun graft.

After implantation, the modified graft promoted full endothelialization after 2 weeks and bare PCL at 4 weeks. It was shown that 80% of the grafts in 2 weeks and 67% of the grafts in 4 weeks demonstrated suppressed cell migration and proliferation entirely within the graft walls due to nitric oxide. After 12 weeks, however, only 40% of the modified grafts revealed no signs of thrombus formation and intimal hyperplasia. In another recent study, Zhang et al.[135] utilized the catalytic ability of Cu^{2+} to generate nitric oxide from endogenous S-nitrosothiols using copper metal−organic framework (MOF) nanoparticles in electrospun polycaprolactone fibers. After 2 weeks in vivo, the bare PCL grafts were barely covered by endothelial cells and had adhered platelets on the luminal surface.

In contrast, the Cu-MOF-modified PCL grafts were almost completely covered with ECs, indicating rapid endothelialization with NO release. SMCs around the bare PCL scaffolds were the α-SMA-positive, synthetic phenotype, and a thinner neointimal hyperplasia formation was seen in the Cu-MOF scaffolds.

Furthermore, the NO generation rate of Cu-MOF scaffolds remained as high as before implantation. Wang et al.[136] used gold nanoparticles as the catalytic agent immobilized on a PET graft by keratin−dopamine conjugates to catalyze NO from S-nitrosoglutathione. Apart from the rapid endothelialization, reduction in HUASMCs' viability and reduced platelet adhesion were noticed for a short period.

Further investigation on the duration of NO generation and in vivo tests need to be conducted for this study to be comparable to other research.[136] Monitoring of the concentration of NO released from a scaffold is crucial to ensure that it is not cytotoxic or causes desensitization of the host tissue. In a human vessels, the range of NO released ranges from 0.5 to 4 $\times 10^{-10}$ mol/cm^2/min.[137]

Another anticoagulant that has been recently used is fucoidan, which is a sulfated polysaccharide isolated from brown algae. Fucoidan has numerous biological properties, including anticoagulant, anti-inflammatory, antioxidant, antibacterial, antiviral, and anticancer properties.[138,139] Yao et al.[139] used fucoidan to modify PVA films for vascular applications. Fucoidan on PVA substantially improves the endothelial cell adhesion and coverage while maintaining the hemocompatibility of PVA. In addition, the in vivo tests exhibited promising results with a higher patency rate and remarkably lower intimal hyperplasia formation for the fucoidan-modified PVA small-diameter grafts. Another anticoagulant that has been used is dextran. It is a polysaccharide with multiple effects in coagulation homeostasis, including the inhibition of platelet activation, diminishing fibrin polymerization, decreasing blood viscosity, and decreasing erythrocyte rouleaux formation that can improve hemocompatibility.[140]

4.1.2.3. Antifouling Agents. Surface functionalization with antifouling agents can elevate the antiadhesive ability of synthetic vascular grafts to improve their overall thromboresistant properties. Increasing the surface wettability to a superhydrophilic surface enables the resistance against protein adsorption. Hydrophilic surfaces resist the adhesion of fouling agents to the material surface through the formation of a physical barrier known as a hydration layer. The most common polymer used for nonfouling in biomedical applications is polyethylene glycol (PEG) and its derivatives. However, PEG is not effective for long-term vascular applications due to its autoxidation when exposed to oxygen and transition metal ions within the blood. Zwitterionic polymers are also known as superhydrophilic and nonfouling materials. They have cationic and anionic moieties on the same chain while the overall charge remains neutral. Zwitterions usually include phosphobetaine, sulfobetaine, and carboxybetaine. Other polymers also used are 2-methacryloyloxyethyl phosphorylcholine (MPC), a custom methacrylate with a zwitterionic phosphorylcholine moiety on the side chain, and poly(2-hydroxyethyl methacrylate) (pHEMA), an FDA-approved biocompatible polymer for soft contact lenses.[141] Various methods have been used for functionalizing the surface, such as spin-coating, surface-initiated atom transfer radical polymerization (SI-ATRP), and covalent bonding.[64] A study by Ji et al.[142] combined the nonfouling properties of carboxybetaine methacrylate with the endothelial cell-selective peptide (REDV). Results showed enhanced hemocompatibility with fewer platelets attached to carboxybetaine-REDV coating and prolonged plasma clotting time than on the uncoated glass surface. A comparison of the adhesion of seeded HUVECs and HUASMCs proved that the REDV peptide helped achieve specific binding of HUVECs. In addition, HUVECs on the modified surface exhibited spreading morphology and reached confluence, whereas HUASMCs on the surface contracted, and no noticeable proliferation was observed. These findings indicate that the use of carboxybetaine methacrylate with REDV might have potential use in promoting rapid endothelialization as well as suppressing the formation of IH.[142]

4.1.2.4. Drug Loading. The addition of pharmaceutical components to a vascular scaffold has been used to enhance the patency of the conduit. Either antithrombotic (acetylsalicylic acid (ASA, aspirin), dipyridamole), antiproliferative (paclitaxel), or bifunctional (cilostazol and clopidogrel) drugs are used for this purpose. Antithrombotic drugs delay platelet adhesion and aggregation on the lumen of the grafts without interfering with the endothelialization process. This is unlike the topical release of antiproliferative drugs, which reduce neointimal formation, and correlated with delayed endothelialization, resulting in an increased risk of thrombosis.[143,144] Various methods have been used to incorporate these drugs in vascular conduits, such as using polymeric substrates for chemical immobilization, coating, and gel beads. However, the most common method by far has been electrospinning with biodegradable polymers to control the dosage and sustained release of the drug into the circulatory system. A study by Punnakitikashem et al.[145] attained a 91 day release of dipyridamole incorporated in an electrospun polyurethane scaffold. Their results showed an increased HAEC viability with increasing concentration of the drug, in contrast to other research.[143] There was also improved nonthrombogenicity and SMC proliferation inhibition with higher doses of dipyridamole.[145] In another study, Yang et al.[54] loaded a PCL electrospun graft with the drug rapamycin (antiproliferative) to combat IH. At 12 weeks, the grafts showed reduced IH without compromising on the re-endothelialization of the grafts.

4.1.3. Effect of Surface Topography. The architecture of a vascular scaffold or graft has a significant impact on the

https://doi.org/10.1021/acsomega.2c01740
ACS Omega 2022, 7, 22125−22148

endothelialization of the conduit. When cells interact with the scaffold or graft, they sense the topography, roughness, microgrooves, ridges, micropores, wells, and nodes of the scaffold, which are then used as directional cues for growth.[163] The scaffold or graft microstructure influences the cell shape, attachment, migration, and proliferation rate, affecting their functionality. Dong et al.[164] conducted a comprehensive study on the effect of topography on the luminal surface of vascular grafts, considering both hemocompatibility and endothelialization. They used PCL as the substrate in the form of nano- and microsized fibers as well as a smooth film surface. The water contact angle was the highest on the nanofibers and lowest on the smooth surface. Most platelets and plasma proteins were adsorbed on the nanofibers, followed by microfibers, with markedly reduced adsorption on the smooth surface. The number of HUVECs adhered to the smooth surface substrates was significantly higher than the number on the other substrates at 2 h. However, there was no difference in the number of adhered HUVECs among the three groups at 6 h. Overall results showed that smooth surface substrates could effectively promote initial HUVEC adhesion, spreading, and proliferation better than the other substrates. Only the cells on the microfibers were spindle-shaped.[164] With contrasting results, Zorlutuna et al.[76] studied the effects of nanopatterned aligned grooves on VSMC cell guidance using collagen type 1 films with parallel channels of equal groove and ridge widths (650 nm by 300 nm depth, 500 nm by 250 nm depth, and 332.5 nm by 200 nm depth). Their results showed that cell adhesion was higher when the pattern dimension was smaller. However, by day 21, the difference in the cell numbers had gradually decreased to a level where there was no appreciable difference with pattern size. Cell adhesion on the nonpatterned films was lower, and there was no orientation of the cells on the films.

The same study by Dong et al.[164] showed that smooth graft surfaces inhibited platelet adhesion and activation, suppressed fibrinogen adsorption, and enhanced EC monolayer formation. An aligned topography aids the direction in which the cells migrate. It produces spindle-shaped ECs, which can be likened to the naturally occurring shape in native arteries. Wang et al.[165] confirmed the aligned formation of resident ECs induced by an aligned nanotopography. The ECs were seeded on a vascular graft with an inner layer fabricated from aligned heparinized silk fibroin and PCL nanofibers. From the given examples above, it can be shown that surface roughness and the presence of physical cues on the graft material and the presence of physical cues on the graft material can affect hemocompatibility and cell behavior, including cell attachment, migration, and proliferation. The processing technique used in the fabrication of a scaffold directly affects the final topography in the luminal layer as well as the spatial required for cell migration. Techniques like electrospinning and hydrogel formation may be manipulated to provide the physical cues for cell adhesion and migration and provide the space required for proliferation.

4.1.3.1. Nanofibrous Structure. Electrospinning has presented itself as a highly favorable method for fabricating vascular grafts due to its versatility and ease of use. Native vessels present ordered multiple structures on the tubular geometry at a macroscopic level and the fibrous architecture at the nanometer scale.[165] Nano- and microdiameter fibers produced by electrospinning mimic the arrangement of connective tissue fibrillar proteins as well as exhibit a large specific surface and high permeability, which is desirable in a biological setting.[35] The porosity and pore sizes in electrospun scaffolds depend on the fiber diameter and their packing density which can be easily controlled by adjusting the properties of the polymer solution and the processing conditions. Despite garnering a reputation for being one of the most favorable fabrication methods for vascular scaffolds or grafts, most electrospun scaffolds often have tiny pores (diameter <6 μm) and low interconnecting porosity, which is a hindrance to cell adhesion, infiltration, and tissue regeneration.[166] However, this can be an advantage, as Gostev et al.[167] with electrospun PU vascular grafts. Results showed that the small pore size of the electrospun grafts hindered the infiltration of blood in the walls and hence blood cells, thereby reducing the risk of leakage and calcification.[167]

In theory, the rate of endothelialization should increase with a nanofibrous surface because a nanofibrous surface mimics the structure of the ECM. However, most researchers report a more rapid endothelialization rate with a microporous structure instead of a nanofibrous structure. Bergmeister et al.[168] studied the effect of graft porosity on cell migration both in vitro and in vivo with fine (2 μm) and coarse mesh (4 μm) electrospun PU grafts. Their results showed that early cell attachment seemed to favor the finer mesh graft over the course mesh in vitro. However, the in vivo study showed that the coarse mesh had cell populations higher than those of the fine mesh. When cell proliferation and infiltration were compared between nanofibrous and microfibrous electrospun structures, the latter showed to be highly favorable. The researchers concluded that it is due to the link between fiber diameter and pore size, where microsized fibers provide a larger surface area for cell attachment, and hence the larger pore size facilitates rapid migration and proliferation of the cells.[169] In contrast, in a study by Yin et al.,[163] ECs seeded on nanoscale fibers showed enhanced cellular orientation and focal adhesion compared to that on microscale fibers. In another investigation by De Valence et al.,[170] there was no difference in the endothelialization rate for the nano- and micro-PCL electrospun fiber sizes of the corresponding porosities (3.3 and 9.1 μm, respectively) of the scaffolds.[163,170]

4.1.3.2. Hydrogel Structure. A hydrogel is a three-dimensional (3D) network system full of water as a dispersion medium. Biological hydrogels possess the advantages of porous structure and high water content, and with adequate cross-linking, they possess viscoelastic properties comparable to those of native arteries.[139] They have been utilized in the field of highly compliant vascular grafts.[171] This structure facilitates rapid endothelialization regardless of the material used. The downside to using hydrogels in the luminal layer is the dislodging of hydrogel particulates, similar to what happens with a thrombus or embolus. The risks involved are stroke, heart attack, and pulmonary embolism.[172] When a hydrogel is used, care has to be taken to ensure minimal damage to the hydrogel occurs.

Most natural materials like gelatin, chitosan, fibrin, and alginate can be made into hydrogel form. One of the most popular synthetic materials processed as a hydrogel is poly(vinyl alcohol) (PVA). PVA is a synthetic, hydrophilic polymer widely used in biomaterial applications. It is produced by polymerization of vinyl acetate to poly(vinyl) acetate followed by hydrolysis of polyvinyl acetate to poly(vinyl alcohol). PVA must be cross-linked in order to be useful for a wide variety of biomedical applications such as contact lenses,

https://doi.org/10.1021/acsomega.2c01740
ACS Omega 2022, 7, 22125−22148

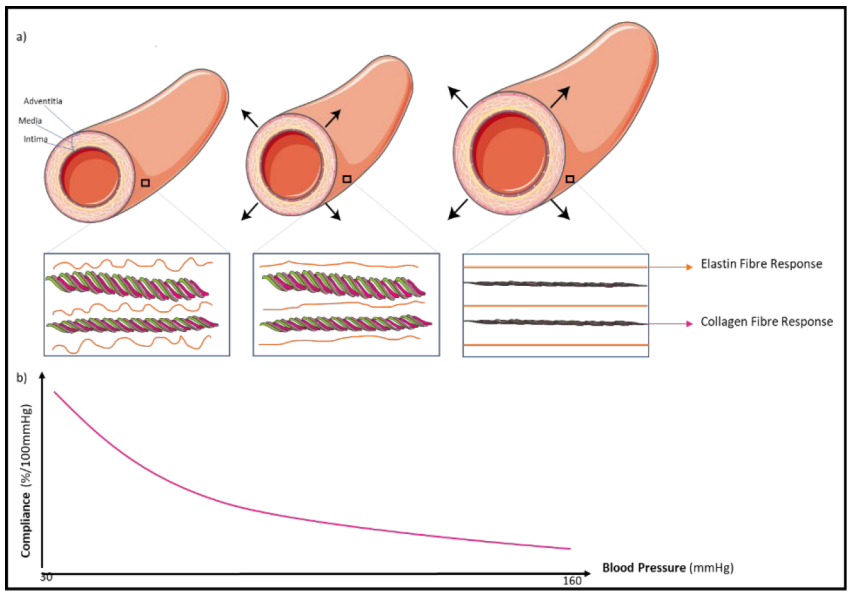

Figure 3. (a) Schematic of arterial response to increasing pressure. (b) Effect on compliance.

wound dressings, local drug delivery systems, and catheters.[140] PVA hydrogels possess good tissue-like elasticity, a highly cross-linked network, and a favorable porous structure, which can deliver active molecules, load cells, and guide tissue remodeling.[173] It has been reported that PVA demonstrated low platelet adhesion and low thrombin generation time.[174] However, PVA hydrogel for a vascular graft showed that the modified PVA with fibronectin, RGDS peptide, cyclicRGD (cRGD) peptide, and heparin showed platelet adhesion similar to that of ePTFE and unmodified PVA. However, the modified PVA had an increased endothelial cell proliferation.[174] Endothelialization of PVA surfaces is a major limitation and can be overcome by modifying biochemical and topographical cues to improve its bioactivity without compromising hemocompatibility. Polypeptides such as fibronectin, peptide (RGDS and cRGD), and lysine, as well as the anticoagulant heparin may be used for this purpose.[173] Although advantageous, porous structures created with different fabrication techniques may have detrimental effects, as well. The following section will discuss the factors to be aware of and the optimal pore structure and size to aim for when fabricating the luminal layer of vascular scaffolds.

4.1.4. Porosity. Porosity and pore size distribution play an important role in the structure and remodeling of a vascular graft. A porous luminal surface plays an important role in stabilizing the intima and aids in the infiltration of cells. It also allows the exchange of nutrients and waste between the seeded cells and the surrounding environment.[169,175] A porous outer surface is also essential as it enhances the penetration of peri-graft tissue, acting as an anchor and inhibiting graft kinking.[118] The pore size that would permit adequate cellular infiltration has been suggested to be greater than 10 μm.[163] A pore size of <10 μm has been reported to hinder cells from entering the scaffold, resulting in a scar plate of collagen and encapsulation of the construct.[176] As pore size and surface area are inversely proportional and cells have been reported to be able to fit themselves and deform to migrate through smaller pore sizes, therefore, the pore size and surface area need to be optimized to ensure that functional cells may regenerate.[177] Different techniques can produce porous structures, including electrospinning, particulate leaching, phase separation, freeze-drying, gas foaming, and 3D printing. Of all these techniques, electrospinning and phase separation are the two facile ways to generate nanofibers in the same size range as the native extracellular matrix.[178]

As much as porosity is encouraged in vascular grafts, a very porous structure can cause adverse effects by allowing penetration of the blood components into the graft walls, leading to entrapment of clot-inducing cells, and ultimately resulting in blood clot formation. This was confirmed by Gupta et al.[179] when they fabricated bilayer grafts from two types of silk: *Antheraea assama* and *Bombyx mori* silk. The inner layer was a very porous structure fabricated (pore size = 5 μm and overall porosity = 90%) using freeze-drying, and the outer layer was made by electrospinning. Their results indicated that one of their grafts experienced acute thrombosis attributed to larger pore sizes.[179]

After all the factors mentioned above have been considered, and a luminal layer with bioactive components that enhances rapid endothelialization and deter platelet adhesion has been successfully fabricated, the fabrication of a mechanically sound second layer may commence. The following section discusses the factors to consider and the work already carried out to create a viscoelastic AVG with compliance matching that of a natural vessel.

4.2. Second Layer (Mechanical Reinforcing Layer). In the dynamic mechanical environment, the artificial graft or scaffold is instantly exposed to pulsatile pressure; thus, a balance between strength and compliance must be achieved. As mentioned before, neither too much nor insufficient compliance in the graft is appropriate to ensure optimal shear stresses within the vessel. Because of the strong correlation between graft compliance and patency of autologous vessels and AVGS, compliance is one of the key areas when designing an AVG.[180] The structure of collagen and elastin determine the mechanical properties of an artery. Elastin fibers (elastic modulus: ~0.6−1 MPa) bear the initial strain imposed by pulsatile pressure. With increasing pressure, the coiled collagen fibers (elastic modulus around ~1 GPa) straighten up and substantially stiffen to bear the increasing

https://doi.org/10.1021/acsomega.2c01740
ACS Omega 2022, 7, 22125−22148

load and protect the vessel from bursting.[181,182] The schematic in Figure 3 shows the response of the arterial wall to increasing pulsatile pressure and its effect on compliance.

Recent research on the mechanical reinforcing layer focuses on utilizing elastomeric materials and biomimicry. In order to match the biomechanical properties of arteries, artificial vascular grafts have to match the nonlinear behavior shown by arteries. Most researchers have been utilizing polymer mixtures of mainly elastomeric and non-elastomeric materials along with combining fabrication techniques. The challenge with this layer is balancing the compliance of the graft to the burst pressure, as these properties are inversely related. Controlling the thickness is one way; however, some properties such as suture retention and kink resistance are sacrificed, as well.[181] This section will focus mainly on biostable polymeric materials or polymers that are known to last for more than 3 months post-implantation in order to maintain the mechanical integrity of the vascular graft.

4.2.1. Elastomeric Biomaterials. Biomaterials, currently being investigated for use in vascular grafts, span a broad range of chemical and mechanical properties but can be broadly categorized as nondegradable and degradable. Nondegradable biomaterials are composed of synthetic polymers of ePTFE, PET, PET, polycarbonate, and polysiloxane-based PUs while slow degrading materials are composed of natural and synthetic polymers such silk, PCL, PLCL, and PU.[39] Degradable materials offer the advantage of allowing the infiltration of cells as the material degrades over time. Despite the theoretical advantages of using degradable materials in vascular grafts, their practical use is considerably limited as the rupture of a VG wall may be a lethal event. Furthermore, an increase in the wall strength synchronous to its degradation at the expense of the newly formed tissue may depend on the patient's state (age, comorbidities, and regenerative capacity).[167] To achieve biomechanical properties which mimic the viscoelastic properties of a human artery, the choice of polymer and their combination, together with the fabrication technique, has profound effects on the resulting properties of the SDAVG. As the target of this review is for SDAVGs targeting the lower limbs, long-term mechanical integrity is also a factor that needs to be addressed.

4.2.1.1. Silk. The properties, structure, and origins of silk have been discussed in the previous sections of this review (4.1.2.1). In the second layer of a vascular graft, silk is mainly used for its slow degradation in vivo, depending on the cross-linking and elasticity.[118] Its mechanical properties depend on the origin of the silk and the processing techniques used. The elasticity and softness of SF are limited due to its highly crystalline β-sheet structure.[41] The construction of the fibers in this layer determines the elasticity of the final structure. Most studies using SF to fabricate vascular conduits use braiding, knitting, gel spinning, or electrospinning techniques to enhance the elasticity and the required strength in the final graft. In an investigation done by Filipe et al.,[183] they fabricated small-diameter vascular grafts from electrospun SF. They evaluated the mechanical properties compared to a commercial ePTFE graft and native rat aorta. Electrospun silk scaffolds revealed a Youngs modulus of 4.2 ± 0.5 MPa, not significantly higher than the native rat aorta (2.1 ± 1.0 MPa) and 7.6-fold more elastic than ePTFE (31.9 ± 1.3 MPa). Ultimate tensile strength results showed that, though silk is not as strong as ePTFE, it is more closely matched to the native rat aorta, reducing problematic compliance mismatch. By investigating the extent of neointimal formation over time and the phenotype of the SMC present, results suggested that hyperplasia stabilized by 6 weeks in SF grafts. Endothelialization is also almost complete, which potentially contributes to the reduced proliferation of SMCs. Contrary to the SF graft, the ePTFE remained uncovered to a great extent, even at 24 weeks.[183] Tanaka et al.[184] prepared an SF vascular graft from a double-raschel knitted mesh with an SF sponge. The longitudinal suture retention strength, circumferential tensile strength, and circumferential compressive elastic modulus of the SF grafts were 6.4 ± 0.6 N, 51.0 ± 3.0 N, and 0.013 ± 0.002 N/mm^2, respectively. These grafts were implanted in the femoral artery of dogs, and results were obtained at 3 months, 5 months, and 1 year post-implantation. Occlusion due to thrombus formation was observed 4 weeks post-implantation in one case. In the remaining five cases, no thrombus formation, intimal hyperplasia, or aneurysm developed.[184] The use of SF as a vascular graft has been proven to increase the patency of the graft by preventing thrombosis as well as IH.

4.2.1.2. Polycaprolactone (PCL). PCL is a hydrophobic, highly crystalline, comparatively elastic polymer with a long degradation time (more than 18 months in vivo). PCL is favorable as a material for vascular grafts as it is nontoxic. However, its hydrophobicity, poor cellular activity, and hypersensitivity to plasma proteins make it unsatisfactory for solo application. With the intent to produce an SDAVG with nonlinear mechanical properties, Ahn et al.[185] fabricated a triple-layered graft with a negative Poisson's ratio (auxetic material). The first layer was made by electrospinning (thickness 200 μm), the second layer (thickness 200 μm) by 3D printing, and the third layer (400 μm) by electrospinning of polycaprolactone. The luminal electrospun layer consisted of nanosized fibers, and the outer layer consisted of microsized fibers. The medial layer was designed to have a negative Poisson's ratio (NPR) or positive Poisson's (PPR) properties. Results showed that the PPR scaffold had a Poisson's ratio of 0.443−0.822 and the NPR graft of 0.750−0.533. The compliance of the NPR and PPR scaffold vascular scaffold was 1.7 times higher and 3.8 times higher than a commercial polytetrafluoroethylene (PTFE) graft, respectively. A limitation of their study was that they did not conduct in vivo studies to determine the patency rate of their grafts compared to commercialized grafts. Furdella et al.[186] measured the compliance of the abdominal aorta of a Sprague−Dawley rat and tested the effect of hypocompliant (Dacron and polytetrafluoroethylene), matched, and hypercompliant electrospun PCL/gelatin graft in vivo. Their results showed that stiff grafts had an increased percentage of endothelialization compared to that of the compliance-matched graft. However, after 28 days in vivo, mechanical stimulus provided by the compliance-matched constructs demonstrated a more favorable cellular environment with increased collagen production in the middle location in the lumen. The hypocompliant grafts showed indications of a proinflammatory environment compared to the other two types of grafts. Despite the favorable remodeling, both the hypercompliant and matched compliant grafts were challenging to handle during implanting and had significantly lower undesirable suture retention than the hypocompliant grafts. Overall, the patency rate was 81% for all types of grafts.

4.2.1.3. Poly(L-lactide-co-ε-caprolactone) (PLCL). The PLCL copolymer comprises a soft matrix of ε-caprolactone moieties and hard domains containing L-lactide units. Poly-

https://doi.org/10.1021/acsomega.2c01740
ACS Omega 2022, 7, 22125−22148

(lactide) is a crystalline hard and brittle material, whereas poly(ε-caprolactone) is a semicrystalline material with rubbery properties. The monomers used in this system differ significantly in mechanical properties and time to reach complete mass loss. However, once physically cross-linked in specific monomer ratios, the system exhibits rubber-like elasticity. The mechanical properties can be adjusted by changing the content of PLLA and PCL. The higher the PCL content, the more elastic and flexible the material is.[41] Using PLCL, Zhang et al.[187] fabricated a triple-layered biomimetic scaffold from PLCL and silk fibroin. The inner layer was fabricated by electrospinning and comprised a more significant amount of PLCL (SF/PLCL = 30/70) to reduce its stiffness. Heparin was also covalently bonded on this luminal layer to further improve the hemocompatibility of the graft. The middle layer had equal amounts or a larger proportion of SF (SF/PLCL = 50/50 or 70/30) to increase the stiffness and create a mechanical gradient similar to that seen in vivo. A braided silk-reinforced tube was chosen as the outer layer to prevent the vascular wall from rupturing. Both grafts had compliance values in the range of the saphenous vein. However, lowering the proportion of PLCL in the middle layer was shown to lower the compliance of the final graft. No tests for SMC proliferation were conducted to determine the effect of compliance on IH. In another study, Kim et al.[188] reported the fabrication of a bilayered PLCL graft by a gel spinning molding technique, resulting in a graft with high tensile strength and high elasticity (550−670% elongation-at-break) and no leakage.

4.2.1.4. Poly(glycerol sebacate) (PGS). PGS is a flexible, nonthrombogenic, biodegradable elastomer produced by polycondensation of glycerol and sebacic acid monomers.[189] Its elastomeric mechanical properties are due to covalent cross-links between random coils and hydrogen bonding between hydroxyl backbone groups.[190] PGS has a superior cellular response to other biodegradable polyesters (e.g., PCL) due to its hydrophilic nature.[176] PGS undergoes complete degradation in vivo within 6 weeks, so it is generally used with other polymers such as PCL.[28]

4.2.1.5. Polyurethane-Based Polymers. Polyurethanes have been used as biomaterials for continuously flexing chronic implants due to their excellent compliant viscoelastic properties. However, their major drawback in such applications has been their variable clinical results and their tendency to degrade uncontrollably, leading to aneurysm formation.[191] The first section of this review paper described the properties and types of PUs used in vascular grafts. PU has high elastic recovery at low strains comparable to arteries; however, arteries tend to display an earlier and more robust strain hardening region at higher strains. Dempsey et al.[180] used a segmented PU to allow elastomeric stretching of the soft segment matrix dominant at low strains followed by the hard domain to combat this problem. As the strain increased, rotation/shear and strain-induced crystallization of the soft segment. They utilized PCU with semi-interpenetrating polymer networks of methacryloxypropyl and (3-acryloxy-2-hydroxypropoxypropyl)-terminated PDMS. Although the resulting graft had compliance levels similar to those of natives, a decrease in burst pressure was also observed. To achieve biomimetic biomechanical properties with PUs, recent research has shown that mixing a highly compliant material such as PU with a stiff material will attain the desired viscoelastic properties that match those of the native artery. In order to mimic the collagen/elastin viscoelastic behavior in arteries, Caracciolo et al.[192] used poly(L-lactic acid) (PLLA) and segmented polyurethane (PHD) to produce an electrospun vascular conduit. Based on the collagen/elastin ratio of muscular arteries, PLLA/PHD 50/50 and 90/10 blend ratios were selected as the SDVG inner and outer layers to mimic native "media" and "adventitia", respectively. The prepared grafts exhibited comparable mechanical behavior under dynamic loading cycles to the greater saphenous vein. Zhang et al.[193] optimized the thickness and homogeneity of the wall in relation to the compliance of an SDAVG by combining wet spun TPU in the first layer, knitted Spandex middle layer, and again TPU spray coating. Although the developed graft had high strength and elasticity, its compliance did not match the native vessels.

To match the nonlinear behavior of arteries and prevent graft leakage, Mi et al.[194] fabricated a triple-layered graft with braided silk fibroin as the inner layer to promote rapid endothelialization, prevent IH, and mimic the collagen behavior at high strain. PAM hydrogel was used as the middle layer to prevent leakage, and the outer layer was made of TPU to mimic the high elasticity of elastin. Their results showed that the introduction of PAM greatly improved the burst pressure. Furthermore, the HUVECs' viability and proliferation rate on the PAM hydrogel were superior to those of the braided silk and TPU, which meant the order of materials would need to be exchanged for optimal endothelialization. The main limitation of this graft was that cells were mainly grown on the surface of the materials due to the dense structure of the overall graft. The mechanical properties closely mimicked the complex behavior of the natural artery, but the presence of suppression of IH was not investigated.

Khodadoust et al.[175] fabricated a vascular graft from PU and PET nanofibers targeting biomimicry of biomechanical properties of arteries. They compared the compliance of electrospun PU, PET and PU/PET hybrid grafts. The PU graft was hypercompliant (∼3 times greater), while the PET graft had lower compliance (∼2 times lower), which was not favorable. The PU/PET graft showed compliance of (4.468 ± 0.177%/0.01 mmHg) in the same range as the saphenous vein.

4.2.2. Structural Factors. 4.2.2.1. Fabrication Method. Various methods are known to enhance the material's elasticity when developing vascular grafts. Such fabrication methods include electrospinning, knitting, braiding, and 3D printing. However, each fabrication technique has disadvantages when used on its own; thus, hybrid structures are employed to impart the required mechanical properties. Electrospinning is very widespread due to its capability to produce a 3D highly porous nanostructure that resembles the ECM and easy adjustment of fabrication parameters, including solution properties, processing variables, ambient conditions, and the type of collector to manipulate the mechanical properties of the final construct[195]—modifying the basic electrospinning setup to achieve biomimetic biomechanical properties of the final developed graft. For example, Akbari et al.[62] used an axially and radially corrugated collector to produce small-diameter vascular grafts with an antikink structure. The major disadvantage of electrospinning is that, in most cases, the final electrospun mat does not possess sufficient mechanical properties to resist the hemodynamic forces experienced after implantation of the graft and leakage of liquid under pressure.[194]

https://doi.org/10.1021/acsomega.2c01740
ACS Omega 2022, 7, 22125−22148

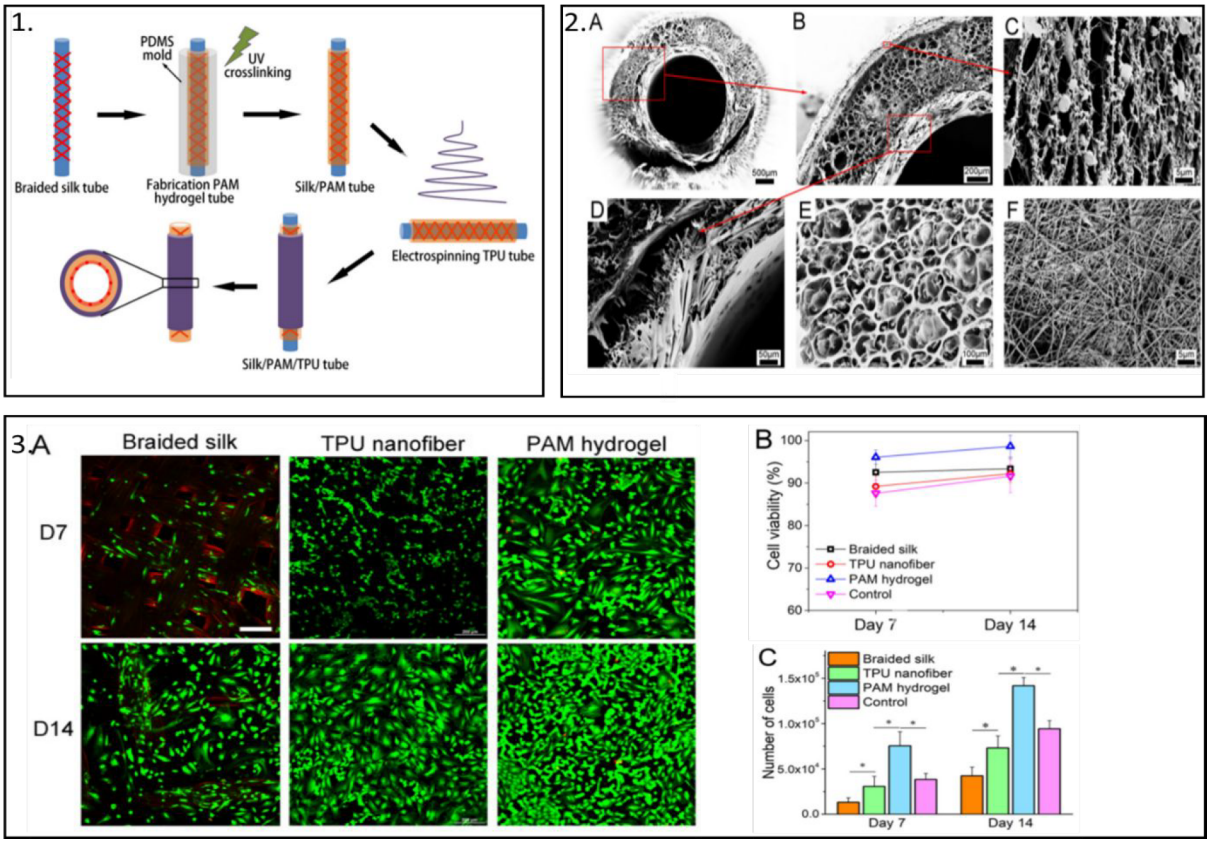

Figure 4. Fabrication and characterization of a triple-layered hybrid graft[194] (1) Schematic illustration of the fabrication procedure (2) (A) Overview of SDVG cross section, (B) enlarged region showing the three layers, (C) cross section of TPU layer, (D) cross section of braided silk and PAM layers, (E) morphology of the inner surface, and (F) morphology of the outer surface. (3) (A) Fluorescence images of HUVECs cultured on braided silk, TPU nanofibers, and the PAM hydrogel from live/dead assays. (B) Cell viability results from live/dead assays. (C) Cell proliferation results from MTS assays. Reprinted in part with permission from ref 194. Copyright 2019 Elsevier.

Knitted structures are well-known for their porosity. The construction can be warp or weft knitted, even though warp knitted structures (double-raschel) are preferred. This type of structure provides the scaffolds with the required porosity; however, one major drawback is the unraveling of the scaffold, leading to aneurysms, fraying at the ends, leakage, and long-term dilation. This was demonstrated in a study by Zhang et al.,[80] where they fabricated a small-diameter graft utilizing collagen as the biomaterial. Their results reported a graft with sufficient porosity to promote cell proliferation. Compliance and burst pressure were comparable to that of the saphenous vein in its dry state. However, the developed graft experienced unraveling and poor mechanical performance in the wet state. Loewen et al.[182] incorporated structural and material elasticity by combining elastic PCU and PVDF in a warp knitted construct. The elastic yarn was fed into the warp knitting machine at a constant thread tension to produce a lock-knit structure. Results showed enhanced compliance values over the pulsatile pressure range, but they were lower than the native vessels. Braided structures are used as a reinforcing layer in most vascular graft constructs. The braiding technique involves using three or more component yarns, which are intertwined at an angle to each other. In other words, braided structures are similar to traditional woven structures but with an angle bias. The angled mesh structure allows easy radial expansion of braided tubes.[28] Grafts developed from both knitting and braiding show nonlinearity with a very low-stress response at low pressures and exhibit a steep increase in elastic modulus as the pressure increases.[196]

Another fabrication technique commonly used is 3D printing, additive manufacturing (AM). 3D printing is a highly versatile technology with precise geometric control which uses lower energy and less time consumption than other techniques. There are several types of AM techniques used in biomedical applications, e.g., selective laser sintering (SLS), direct ink writing (DIW), stereolithography (SLA), fused deposition modeling (FDM) or fused filament fabrication (FFF), and bioprinting technologies.[197] By combining two types of additive manufacturing techniques, Byrne et al.[181] proposed a design of a three-layered graft, with the inner layer serving as an impermeable low stiffness matrix (100% modulus: 55.2 kPa) to mimic the role of elastin fabricated by direct ink writing of soft room temperature vulcanized silicone. A fiber reinforcing layer is designed to slack at low pressure and become taut as the mean pressure is increased and incorporated by fused filament fabrication. The final encapsulation layer ensured that the underlying layers expanded and contracted in unison under cyclic loading. The investigation using finite element analysis and tensile tests produced a range of compliance results that would allow the fabrication of patient-specific grafts in compliance. Casting/molding is another standard method used in early research or as the luminal layer in VGs. It involves dissolving a polymer in a solvent or melting it and using a mold to form the required shape. The mechanical properties of the cast scaffold or graft

https://doi.org/10.1021/acsomega.2c01740
ACS Omega 2022, 7, 22125−22148

are not as good as other grafts; therefore, different fabrication methods are combined with the casting method to form a hybrid structure.[198] An example of the fabrication and results obtained with a trilayered SDVG is shown in Figure 4.

4.2.2.2. Controlling Porosity. Porosity in a vascular graft affects cell adhesion, migration, and proliferation, as well as the mechanical integrity of the graft. Highly porous structures with interconnected cavities are crucial as they support cell growth and facilitate the uniform distribution of cells. However, it reduces the overall strength of the graft. The mechanical strength and porosity have to be optimized in order to achieve an optimal balance between the two. For instance, in a study by Soliman et al.,[169] the mechanical properties of the grafts decreased with an increase in porosity. Highly porous structures can also lead to the leakage of blood into the surrounding tissue. Thus, the compromise between optimal tissue regeneration, low blood leakage, and adequate mechanical properties is challenging to achieve with a homogeneous construct. However, it could be addressed with multilayered vascular grafts.[170] Chan et al.[200] studied the effect of significantly varying fiber diameters (355 ± 5 nm vs 2750 ± 61 nm) and their corresponding interconnected porosity (23.3 ± 1.7% vs 45.1 ± 1.2%) and the solvent (water vs HFIP) used on the mechanical properties of an SF graft.

Increasing the diameter of the fibers resulted in a much stiffer graft with a higher burst pressure and suture retention strength. Increasing the porosity of the graft resulted in an increased rate of endothelialization. The difference in fiber diameter between the nano- and microsized fiber influenced the neointimal growth rate in such a way that for the nanosized fibers, there was a sharp increase from week 3 to week 6 followed by contraction to a stable level, whereas the microsized fibers showed a gradual increase from week 3 all the way to week 24. Microsilk elicited a significantly earlier contractile SMC phenotype switch compared to nanosilk. In addition, it contributed to the steady neointimal hyperplasia progression and lower stabilization levels of neointimal hyperplasia at later time points.[199] Using gel spinning, Rodriguez et al.[119] fabricated a vascular conduit from a low concentration silk solution with optimized porosity and mechanical properties. The fabricated grafts showed compliance values (3.3 mmHg × 10^{-2}) comparable to those of the saphenous vein in vitro, and increasing the porosity also increased the cell colonization rate. The less porous grafts inhibited cell growth and resulted in failure of the material to degrade. In vivo, when the grafts were implanted in the abdominal aorta of Sprague−Dawley rats, none of the highly porous tubes remained patent after 6 months, which was said to be due to mechanical failure or a compromised interface between the blood and the surface of the tubes.[120]

5. CONCLUSION

To overcome the challenges currently being encountered with the available grafts concerning IH, developing a biomimetic AVG is one of the solutions. The fabrication of multilayered grafts with a designated function for each layer will help overcome some of these issues. This review focused on developing a biomimetic SDVG for peripheral applications such as femoropopliteal bypass to overcome intimal hyperplasia. For such a purpose, length and slow degrading polymers or biostability are prerequisites and other requirements for a vascular graft. First, the limitations and advantages of the current AVGs such as the PET (Dacron), ePTFE (Gore-Tex), and PU grafts were discussed. The triggers of IH, such as bioincompatibility and mismatch in biomechanical properties, were then explained. Like in the native artery, each layer in a multilayered graft has a different requirement depending on the function.

In contact with the blood, the lumen layer requires rapid endothelialization, nonimmunogenicity, and nontoxicity and should allow the passage of nutrients and waste but no other blood components. This can be done by creating biological or physical cues to promote rapid endothelialization of the graft and provide sufficient interconnected porosity. The use of natural biomaterials, which contain ligands that bind with receptors on cells, is one way, but the nonspecificity of the cells is still a challenge. Natural biomaterials encourage endothelialization; however, they come with challenges that trigger IH. A comparison of various ECM-derived polymers like collagen, laminin, fibrin, hyaluronic acid, and other natural polymers such as silk and chitosan on promoting endothelialization and SMC adhesion, migration, and proliferation was done. Combining other compounds such as anticoagulants and superhydrophilic polymers with these natural polymers in the luminal layer is also used to deter nonspecific protein and platelet adhesion. The second and any other layers to be added are required to provide mechanical integrity to the graft as well as prevent the leakage of blood constituents in the surrounding tissues. To prevent biomechanical mismatch, to be more specific, a compliance mismatch between the native vessel and the artificial graft, nonlinearity in response to pulsatile pressure, is crucial. For this purpose, elastomeric and non-elastomeric polymers with an appropriate fabrication technique such as electrospinning, 3D printing, braiding, knitting, and casting may achieve this aim. With these techniques, a balance between the burst pressure, compliance, porosity, and ultimate tensile strength also needs to be met. Although an ideal, patient-specific artificial graft to replace diseased arteries is still yet to be fabricated, current research has shown that a biomimetic artificial graft is possible. The use of imaging techniques such as magnetic resonance imaging (MRI) and Doppler ultrasound to measure patient parameters and utilize these parameters in computational fluid dynamic brings research a step closer to patient specificity.

AUTHOR INFORMATION

Corresponding Author

Shadi Houshyar − *School of Engineering, RMIT University, Melbourne 3000, Australia;* orcid.org/0000-0003-0288-8608; Email: shadi.houshyar@rmit.edu.au

Authors

Rumbidzai Zizhou − *Center for Materials Innovation and Future Fashion (CMIFF), School of Fashion and Textiles, RMIT University, Brunswick 3056, Australia*

Xin Wang − *Center for Materials Innovation and Future Fashion (CMIFF), School of Fashion and Textiles, RMIT University, Brunswick 3056, Australia;* orcid.org/0000-0003-0862-9631

Complete contact information is available at: https://pubs.acs.org/10.1021/acsomega.2c01740

Notes

The authors declare no competing financial interest.

https://doi.org/10.1021/acsomega.2c01740
ACS Omega 2022, 7, 22125−22148

■ ACKNOWLEDGMENTS

The authors would like to acknowledge RMIT University RRSS-SC scholarship for providing the funding to make this paper possible. S.H. acknowledges the funding support through the RMIT Vice-Chancellor's Research Fellowship.

■ REFERENCES

(1) Weber, C.; Reinhardt, S.; Eghbalzadeh, K.; Wacker, M.; Guschlbauer, M.; Maul, A.; Sterner-Kock, A.; Wahlers, T.; Wippermann, J.; Scherner, M. Patency and in vivo compatibility of bacterial nanocellulose grafts as small-diameter vascular substitute. *J. Vasc. Surg.* **2018**, *68* (6), 177S−187S.

(2) Mobin-Uddin, K.; Vincent, G. S.; Evans, W. E. Prevention of anastomotic intimal hyperplasia in infrainguinal PTFE bypass grafts with distal arterial segment interposition. *Vasc. surg.* **1999**, *33* (3), 269−281.

(3) Pennings, I.; van Haaften, E. E.; Jungst, T.; Bulsink, J. A.; Rosenberg, A. J.; Groll, J.; Bouten, C. V.; Kurniawan, N. A.; Smits, A. I.; Gawlitta, D. Layer-specific cell differentiation in bi-layered vascular grafts under flow perfusion. *Biofabrication* **2020**, *12* (1), 015009.

(4) Fernández-Colino, A.; Wolf, F.; Rütten, S.; Schmitz-Rode, T.; Rodríguez-Cabello, J. C.; Jockenhoevel, S.; Mela, P. Small caliber compliant vascular grafts based on elastin-like recombinamers for in situ tissue engineering. *Front. Bioeng. Biotechnol.* **2019**, *7*, 340.

(5) Zhuang, Y.; Zhang, C.; Cheng, M.; Huang, J.; Liu, Q.; Yuan, G.; Lin, K.; Yu, H. Challenges and strategies for in situ endothelialization and long-term lumen patency of vascular grafts. *Bioact. Mater.* **2021**, *6* (6), 1791−1809.

(6) Greenwald, S.; Berry, C. Improving vascular grafts: the importance of mechanical and haemodynamic properties. *J. Pathol.* **2000**, *190* (3), 292−299.

(7) Guan, G.; Yu, C.; Xing, M.; Wu, Y.; Hu, X.; Wang, H.; Wang, L. Hydrogel small-diameter vascular graft reinforced with a braided fiber strut with improved mechanical properties. *Polymers* **2019**, *11* (5), 810.

(8) Prichard, H. L.; Manson, R. J.; DiBernardo, L.; Niklason, L. E.; Lawson, J. H.; Dahl, S. L. An early study on the mechanisms that allow tissue-engineered vascular grafts to resist intimal hyperplasia. *J. Cardiovasc. Transl. Res.* **2011**, *4* (5), 674−682.

(9) Ward, A. O.; Caputo, M.; Angelini, G. D.; George, S. J.; Zakkar, M. Activation and inflammation of the venous endothelium in vein graft disease. *Atherosclerosis* **2017**, *265*, 266−274.

(10) Pennel, T.; Zilla, P. Clinical Applications and Limitations of Vascular Grafts. *Tissue-Engineered Vascu. Grafts* **2020**, 3−34.

(11) Abdollahi, S.; Boktor, J.; Hibino, N. Bioprinting of freestanding vascular grafts and the regulatory considerations for additively manufactured vascular prostheses. *Transl. Res.* **2019**, *211*, 123−138.

(12) Mueller, K.-M.; Dasbach, G. The pathology of vascular grafts. *Pathol. Devices* **1994**, *86*, 273−306.

(13) Shimada, T.; Nishibe, T.; Miura, H.; Hazama, K.; Kato, H.; Kudo, F.; Murashita, T.; Okuda, Y. Improved healing of small-caliber, long-fibril expanded polytetrafluoroethylene vascular grafts by covalent bonding of fibronectin. *Surg. Today* **2004**, *34* (12), 1025−1030.

(14) Zilla, P.; Bezuidenhout, D.; Human, P. Prosthetic vascular grafts: wrong models, wrong questions and no healing. *Biomaterials* **2007**, *28* (34), 5009−5027.

(15) Chlupáč, J.; Filova, E.; Bačáková, L. Blood vessel replacement: 50 years of development and tissue engineering paradigms in vascular surgery. *Physiol. Res. (Prague, Czech Repub.)* **2009**, *58* (Suppl2), S119−S139.

(16) Bui, H. T.; Friederich, A. R.; Li, E.; Prawel, D. A.; James, S. P. Hyaluronan enhancement of expanded polytetrafluoroethylene cardiovascular grafts. *J. Biomater. Appl.* **2018**, *33* (1), 52−63.

(17) Sarkar, S.; Salacinski, H.; Hamilton, G.; Seifalian, A. The mechanical properties of infrainguinal vascular bypass grafts: their role in influencing patency. *Eur. J. Vasc. Endovasc. Surg.* **2006**, *31* (6), 627−636.

(18) Wise, S. G.; Liu, H.; Kondyurin, A.; Byrom, M. J.; Bannon, P. G.; Edwards, G. A.; Weiss, A. S.; Bao, S.; Bilek, M. M. Plasma ion activated expanded polytetrafluoroethylene vascular grafts with a covalently immobilized recombinant human tropoelastin coating reducing neointimal hyperplasia. *ACS Biomater. Sci. Eng.* **2016**, *2* (8), 1286−1297.

(19) Bosiers, M.; Deloose, K.; Verbist, J.; Schroë, H.; Lauwers, G.; Lansink, W.; Peeters, P. Heparin-bonded expanded polytetrafluoroethylene vascular graft for femoropopliteal and femorocrural bypass grafting: 1-year results. *J. Vasc. Surg.* **2006**, *43* (2), 313−318.

(20) Toes, G.; Van Muiswinkel, K.; Van Oeveren, W.; Suurmeijer, A.; Timens, W.; Stokroos, I.; Van den Dungen, J. Superhydrophobic modification fails to improve the performance of small diameter expanded polytetrafluoroethylene vascular grafts. *Biomaterials* **2002**, *23* (1), 255−262.

(21) Zhang, J.; Huang, H.; Ju, R.; Chen, K.; Li, S.; Wang, W.; Yan, Y. In vivo biocompatibility and hemocompatibility of a polytetrafluoroethylene small diameter vascular graft modified with sulfonated silk fibroin. *Am. J. Surg.* **2017**, *213* (1), 87−93.

(22) Bowlin, G. L.; Meyer, A.; Fields, C.; Cassano, A.; Makhoul, R. G.; Allen, C.; Rittgers, S. E. The persistence of electrostatically seeded endothelial cells lining a small diameter expanded polytetrafluoroethylene vascular graft. *J. Biomater. Appl.* **2001**, *16* (2), 157−173.

(23) Mi, H.-Y.; Jing, X.; Thomsom, J. A.; Turng, L.-S. Promoting endothelial cell affinity and antithrombogenicity of polytetrafluoroethylene (PTFE) by mussel-inspired modification and RGD/heparin grafting. *J. Mater. Chem. B* **2018**, *6* (21), 3475−3485.

(24) Jafari, S.; Hosseini Salekdeh, S. S.; Solouk, A.; Yousefzadeh, M. Electrospun polyethylene terephthalate (PET) nanofibrous conduit for biomedical application. *Polym. Adv. Technol.* **2020**, *31* (2), 284−296.

(25) Rahmati Nejad, M.; Yousefzadeh, M.; Solouk, A. Electrospun PET/PCL small diameter nanofibrous conduit for biomedical application. *Mater. Sci. Eng. C* **2020**, *110*, 110692.

(26) Pezzoli, D.; Cauli, E.; Chevallier, P.; Fare, S.; Mantovani, D. Biomimetic coating of cross-linked gelatin to improve mechanical and biological properties of electrospun PET: A promising approach for small caliber vascular graft applications. *J. Biomed. Mater. Res., Part A* **2017**, *105* (9), 2405−2415. Dimitrievska, S.; Maire, M.; Diaz-Quijada, G. A.; Robitaille, L.; Ajji, A.; Yahia, L. H.; Moreno, M.; Merhi, Y.; Bureau, M. N. Low thrombogenicity coating of nonwoven PET fiber structures for vascular grafts. *Macromol. Biosci.* **2011**, *11* (4), 493−502.

(27) Tanaka, T.; Tanaka, R.; Ogawa, Y.; Takagi, Y.; Asakura, T. Development of small-diameter polyester vascular grafts coated with silk fibroin sponge. *Organogenesis* **2020**, *16* (1), 1−13.

(28) Singh, C.; Wong, C. S.; Wang, X. Medical textiles as vascular implants and their success to mimic natural arteries. *J. Funct. Biomater.* **2015**, *6* (3), 500−525.

(29) Hong, Y.; Guan, J.; Fujimoto, K. L.; Hashizume, R.; Pelinescu, A. L.; Wagner, W. R. Tailoring the degradation kinetics of poly (ester carbonate urethane) urea thermoplastic elastomers for tissue engineering scaffolds. *Biomaterials* **2010**, *31* (15), 4249−4258.

(30) Qiu, X.; Lee, B. L.-P.; Ning, X.; Murthy, N.; Dong, N.; Li, S. End-point immobilization of heparin on plasma-treated surface of electrospun polycarbonate-urethane vascular graft. *Acta Biomater.* **2017**, *51*, 138−147.

(31) Khan, M.; Yang, J.; Shi, C.; Lv, J.; Feng, Y.; Zhang, W. Surface tailoring for selective endothelialization and platelet inhibition via a combination of SI-ATRP and click chemistry using Cys-Ala-Gly-peptide. *Acta Biomater.* **2015**, *20*, 69−81.

(32) Gostev, A. A.; Karpenko, A. A.; Laktionov, P. P. Polyurethanes in cardiovascular prosthetics. *Polym. Bull.* **2018**, *75* (9), 4311−4325.

(33) Gradinaru, L.; Ciobanu, C.; Vlad, S.; Drobota, M.; Butnaru, M.; Saint-Pierre, G. Thermal behavior, surface energy analysis, and hemocompatibility of some polycarbonate urethanes for cardiac engineering. *High Perform. Polym.* **2015**, *27* (5), 637−645.

(34) Kannan, R. Y.; Salacinski, H. J.; Sales, K. M.; Butler, P. E.; Seifalian, A. M. The endothelization of polyhedral oligomeric

https://doi.org/10.1021/acsomega.2c01740
ACS Omega 2022, 7, 22125−22148

silsesquioxane nanocomposites. *Cell Biochem. Biophys.* **2006**, *45* (2), 129−136.
(35) Ong, C. S.; Zhou, X.; Huang, C. Y.; Fukunishi, T.; Zhang, H.; Hibino, N. Tissue engineered vascular grafts: current state of the field. *Expert Rev. Med. Devices* **2017**, *14* (5), 383−392.
(36) AbuRahma, A. F. Overview of noninvasive vascular techniques in peripheral arterial disease. *Noninvasive Peripheral Arterial Diagnosis*; Springer, 2010; pp 15−24.
(37) Newby, A. C.; Zaltsman, A. B. Molecular mechanisms in intimal hyperplasia. *J. Pathol.* **2000**, *190* (3), 300−309.
(38) Tu, C.; Das, S.; Baker, A. B.; Zoldan, J.; Suggs, L. J. Nanoscale strategies: treatment for peripheral vascular disease and critical limb ischemia. *ACS Nano* **2015**, *9* (4), 3436−3452.
(39) Liu, R. H.; Ong, C. S.; Fukunishi, T.; Ong, K.; Hibino, N. Review of vascular graft studies in large animal models. *Tissue Eng., Part B* **2018**, *24* (2), 133−143.
(40) Zheng, W.; Wang, Z.; Song, L.; Zhao, Q.; Zhang, J.; Li, D.; Wang, S.; Han, J.; Zheng, X.-L.; Yang, Z.; Kong, D. Endothelialization and patency of RGD-functionalized vascular grafts in a rabbit carotid artery model. *Biomaterials* **2012**, *33* (10), 2880−2891.
(41) Li, X.; Zhao, H. Mechanical and degradation properties of small-diameter vascular grafts in an in vitro biomimetic environment. *J. Biomater. Appl.* **2019**, *33* (8), 1017−1034.
(42) Lemson, M.; Tordoir, J.; Daemen, M.; Kitslaar, P. Intimal hyperplasia in vascular grafts. *European J. Vasc. Endovasc. Surg.* **2000**, *19* (4), 336−350.
(43) KRuGER, D. Neo-intimal hyperplasia, diabetes and endovascular injury. *Cardiovasc. J. Afr.* **2012**, *23* (9), 507.
(44) Jeong, Y.; Yao, Y.; Yim, E. K. Current understanding of intimal hyperplasia and effect of compliance in synthetic small diameter vascular grafts. *Biomater. Sci.* **2020**, *8* (16), 4383−4395.
(45) Tseng, C.-N.; Karlöf, E.; Chang, Y.-T.; Lengquist, M.; Rotzius, P.; Berggren, P.-O.; Hedin, U.; Eriksson, E. E. Contribution of endothelial injury and inflammation in early phase to vein graft failure: the causal factors impact on the development of intimal hyperplasia in murine models. *PLoS One* **2014**, *9* (6), No. e98904.
(46) Haruguchi, H.; Teraoka, S. Intimal hyperplasia and hemodynamic factors in arterial bypass and arteriovenous grafts: a review. *J. Artif. Organs* **2003**, *6* (4), 227−235.
(47) Kijani, S.; Vázquez, A. M.; Levin, M.; Borén, J.; Fogelstrand, P. Intimal hyperplasia induced by vascular intervention causes lipoprotein retention and accelerated atherosclerosis. *Physiol. Rep.* **2017**, *5* (14), No. e13334.
(48) Rotmans, J. I.; Velema, E.; Verhagen, H. J.; Blankensteijn, J. D.; de Kleijn, D. P.; Stroes, E. S.; Pasterkamp, G. Matrix metalloproteinase inhibition reduces intimal hyperplasia in a porcine arteriovenous-graft model. *J. Vasc. Surg.* **2004**, *39* (2), 432−439.
(49) He, Y.; Fernandez, C. M.; Jiang, Z.; Tao, M.; O'Malley, K. A.; Berceli, S. A. Flow reversal promotes intimal thickening in vein grafts. *J. Vasc. Surg.* **2014**, *60* (2), 471−478.
(50) Meirson, T.; Orion, E.; Di Mario, C.; Webb, C.; Patel, N.; Channon, K. M.; Ben Gal, Y.; Taggart, D. P. Flow patterns in externally stented saphenous vein grafts and development of intimal hyperplasia. *J. Thorac. Cardiovasc. Surg.* **2015**, *150* (4), 871−879.
(51) Post, A.; Diaz-Rodriguez, P.; Balouch, B.; Paulsen, S.; Wu, S.; Miller, J.; Hahn, M.; Cosgriff-Hernandez, E. Elucidating the role of graft compliance mismatch on intimal hyperplasia using an ex vivo organ culture model. *Acta Biomater.* **2019**, *89*, 84−94.
(52) Verrier, E. D.; Boyle Jr, E. M. Endothelial cell injury in cardiovascular surgery. *Annals Thorac. Surg.* **1996**, *62* (3), 915−922.
(53) Sur, S.; Sugimoto, J. T.; Agrawal, D. K. Coronary artery bypass graft: why is the saphenous vein prone to intimal hyperplasia? *Can. J. Physiol. Pharmacol.* **2014**, *92* (7), 531−545.
(54) Yang, Y.; Lei, D.; Zou, H.; Huang, S.; Yang, Q.; Li, S.; Qing, F.-L.; Ye, X.; You, Z.; Zhao, Q. Hybrid electrospun rapamycin-loaded small-diameter decellularized vascular grafts effectively inhibit intimal hyperplasia. *Acta Biomater.* **2019**, *97*, 321−332.
(55) Bouchet, M.; Gauthier, M.; Maire, M.; Ajji, A.; Lerouge, S. Towards compliant small-diameter vascular grafts: predictive analytical model and experiments. *Mater. Sci. Eng., Part C* **2019**, *100*, 715−723.
(56) Eilenberg, M.; Enayati, M.; Ehebruster, D.; Grasl, C.; Walter, I.; Messner, B.; Baudis, S.; Potzmann, P.; Kaun, C.; Podesser, B. K.; Wojta, J.; Bergmeister, H. Long term evaluation of nanofibrous, bioabsorbable polycarbonate urethane grafts for small diameter vessel replacement in rodents. *Eur. J. Vasc. Endovasc. Surg.* **2020**, *59* (4), 643−652.
(57) Gao, J.; Guo, H.; Tian, S.; Qiao, Y.; Han, J.; Li, Y.; Wang, L. Preparation and mechanical performance of small-diameter PHBHHx vascular graft by electrospinning. *Int. J. Polym. Mater. Polym. Biomater.* **2019**, *68* (10), 575−581.
(58) Tai, N.; Salacinski, H.; Edwards, A.; Hamilton, G.; Seifalian, A. Compliance properties of conduits used in vascular reconstruction. *Br. J. Surg.* **2002**, *87* (11), 1516−1524.
(59) van Uden, S.; Vanerio, N.; Catto, V.; Bonandrini, B.; Tironi, M.; Figliuzzi, M.; Remuzzi, A.; Kock, L.; Redaelli, A. C L; Greco, F. G; Riboldi, S. A A novel hybrid silk-fibroin/polyurethane three-layered vascular graft: towards in situ tissue-engineered vascular accesses for haemodialysis. *Biomed. Mater.* **2019**, *14* (2), 025007.
(60) Montini-Ballarin, F.; Calvo, D.; Caracciolo, P. C.; Rojo, F.; Frontini, P. M.; Abraham, G. A.; Guinea, G. V. Mechanical behavior of bilayered small-diameter nanofibrous structures as biomimetic vascular grafts. *J. Mech. Behav. Biomed. Mater.* **2016**, *60*, 220−233.
(61) Gui, L.; Boyle, M. J.; Kamin, Y. M.; Huang, A. H.; Starcher, B. C.; Miller, C. A.; Vishnevetsky, M. J.; Niklason, L. E. Construction of tissue-engineered small-diameter vascular grafts in fibrin scaffolds in 30 days. *Tissue Eng., Part A* **2014**, *20* (9−10), 1499−1507.
(62) Akbari, S.; Mohebbi-Kalhori, D.; Samimi, A. Effect of corrugated structure on the collapsing of the small-diameter vascular scaffolds. *J. Biomater. Appl.* **2020**, *34* (10), 1355−1367.
(63) Salacinski, H. J.; Goldner, S.; Giudiceandrea, A.; Hamilton, G.; Seifalian, A. M.; Edwards, A.; Carson, R. J. The mechanical behavior of vascular grafts: a review. *J. Biomater. Appl.* **2001**, *15* (3), 241−278.
(64) Zhu, T.; Gu, H.; Zhang, H.; Wang, H.; Xia, H.; Mo, X.; Wu, J. Covalent grafting of PEG and heparin improves biological performance of electrospun vascular grafts for carotid artery replacement. *Acta Biomater.* **2021**, *119*, 211−224.
(65) Adipurnama, I.; Yang, M.-C.; Ciach, T.; Butruk-Raszeja, B. Surface modification and endothelialization of polyurethane for vascular tissue engineering applications: a review. *Biomater. Sci.* **2017**, *5* (1), 22−37.
(66) Pawlowski, K. J.; Rittgers, S. E.; Schmidt, S. P.; Bowlin, G. L. Endothelial cell seeding of polymeric vascular grafts. *Front. Biosci.* **2004**, *9* (1−3), 1412.
(67) Noel, S.; Fortier, C.; Murschel, F.; Belzil, A.; Gaudet, G.; Jolicoeur, M.; De Crescenzo, G. Co-immobilization of adhesive peptides and VEGF within a dextran-based coating for vascular applications. *Acta Biomater.* **2016**, *37*, 69−82.
(68) Neufurth, M.; Wang, X.; Tolba, E.; Dorweiler, B.; Schröder, H. C.; Link, T.; Diehl-Seifert, B.; Müller, W. E. Modular small diameter vascular grafts with bioactive functionalities. *PloS one* **2015**, *10* (7), No. e0133632.
(69) Wang, Y.; Chen, S.; Pan, Y.; Gao, J.; Tang, D.; Kong, D.; Wang, S. Rapid in situ endothelialization of a small diameter vascular graft with catalytic nitric oxide generation and promoted endothelial cell adhesion. *J. Mater. Chem., Part B* **2015**, *3* (47), 9212−9222.
(70) Yuan, H.; Chen, C.; Liu, Y.; Lu, T.; Wu, Z. Strategies in cell-free tissue-engineered vascular grafts. *J. Biomed. Mater. Res., Part A* **2020**, *108* (3), 426−445.
(71) Chernonosova, V. S.; Gostev, A. A.; Chesalov, Y. A.; Karpenko, A. A.; Karaskov, A. M.; Laktionov, P. P. Study of hemocompatibility and endothelial cell interaction of tecoflex-based electrospun vascular grafts. *Int. J. Polym. Mater. Polym. Biomater.* **2019**, *68* (1−3), 34−43.
(72) Wise, S. G.; Waterhouse, A.; Michael, P.; Ng, M. K. Extracellular matrix molecules facilitating vascular biointegration. *J. Funct. Biomater.* **2012**, *3* (3), 569−587.

https://doi.org/10.1021/acsomega.2c01740
ACS Omega 2022, 7, 22125−22148

(73) Gomes, S.; Leonor, I. B.; Mano, J. F.; Reis, R. L.; Kaplan, D. L. Natural and genetically engineered proteins for tissue engineering. *Prog. Polym. Sci.* **2012**, *37* (1), 1−17.
(74) Goh, E. T.; Wong, E.; Farhatnia, Y.; Tan, A.; Seifalian, A. M. Accelerating in situ endothelialisation of cardiovascular bypass grafts. *Int. J. Mol. Sci.* **2015**, *16* (1), 597−627.
(75) Wertheimer, S.; Sharabi, M.; Shelah, O.; Lesman, A.; Haj-Ali, R. Bio-composites reinforced with unique coral collagen fibers: Towards biomimetic-based small diameter vascular grafts. *J. Mech. Behav. Biomed. Mater.* **2021**, *119*, 104526.
(76) Zorlutuna, P.; Elsheikh, A.; Hasirci, V. Nanopatterning of collagen scaffolds improve the mechanical properties of tissue engineered vascular grafts. *Biomacromolecules* **2009**, *10* (4), 814−821.
(77) Wong, C. S.; Liu, X.; Xu, Z.; Lin, T.; Wang, X. Elastin and collagen enhances electrospun aligned polyurethane as scaffolds for vascular graft. *J. Mater. Sci.: Mater. Med.* **2013**, *24* (8), 1865−1874.
(78) Lambert, L.; Novakova, M.; Lukac, P.; Cechova, D.; Sukenikova, L.; Hrdy, J.; Mlcek, M.; Chlup, H.; Suchy, T.; Grus, T. Evaluation of the immunogenicity of a vascular graft covered with collagen derived from the European carp (Cyprinus carpio) and bovine collagen. *BioMed. Res. Int.* **2019**, *2019*, 5301405.
(79) Ryan, A. J.; Ryan, E. J.; Cameron, A. R.; O'Brien, F. J. Hierarchical biofabrication of biomimetic collagen-elastin vascular grafts with controllable properties via lyophilisation. *Acta Biomater.* **2020**, *112*, 52−61.
(80) Zhang, F.; Xie, Y.; Celik, H.; Akkus, O.; Bernacki, S. H.; King, M. W. Engineering small-caliber vascular grafts from collagen filaments and nanofibers with comparable mechanical properties to native vessels. *Biofabrication* **2019**, *11* (3), 035020.
(81) Kumar, V. A.; Caves, J. M.; Haller, C. A.; Dai, E.; Liu, L.; Grainger, S.; Chaikof, E. L. Acellular vascular grafts generated from collagen and elastin analogs. *Acta Biomater.* **2013**, *9* (9), 8067−8074.
(82) Koens, M.; Krasznai, A.; Hanssen, A.; Hendriks, T.; Praster, R.; Daamen, W.; Van Der Vliet, J.; Van Kuppevelt, T. Vascular replacement using a layered elastin-collagen vascular graft in a porcine model: one week patency versus one month occlusion. *Organogenesis* **2015**, *11* (3), 105−121.
(83) Wise, S. G.; Byrom, M. J.; Waterhouse, A.; Bannon, P. G.; Ng, M. K.; Weiss, A. S. A multilayered synthetic human elastin/polycaprolactone hybrid vascular graft with tailored mechanical properties. *Acta Biomater.* **2011**, *7* (1), 295−303.
(84) Matsuura, S.; Takayama, T.; Oyama, T. G.; Oyama, K.; Taguchi, M.; Endo, T.; Akai, T.; Isaji, T.; Hoshina, K. A Radiation-Crosslinked Gelatin Hydrogel That Promotes Tissue Incorporation of an Expanded Polytetrafluoroethylene Vascular Graft in Rats. *Biomolecules* **2021**, *11* (8), 1105.
(85) Lamprou, D.; Zhdan, P.; Labeed, F.; Lekakou, C. Gelatine and gelatine/elastin nanocomposites for vascular grafts: processing and characterization. *J. Biomater. Appl.* **2011**, *26* (2), 209−226.
(86) Joy, J.; Pereira, J.; Aid-Launais, R.; Pavon-Djavid, G.; Ray, A. R.; Letourneur, D.; Meddahi-Pellé, A.; Gupta, B. Electrospun micro-porous gelatin-polycaprolactone blend tubular scaffold as a potential vascular biomaterial. *Polym. Int.* **2019**, *68* (7), 1367−1377.
(87) Shalumon, K.; Deepthi, S.; Anupama, M.; Nair, S.; Jayakumar, R.; Chennazhi, K. Fabrication of poly (l-lactic acid)/gelatin composite tubular scaffolds for vascular tissue engineering. *Int. J. Biol. Macromol.* **2015**, *72*, 1048−1055.
(88) Nagiah, N.; Johnson, R.; Anderson, R.; Elliott, W.; Tan, W. Highly compliant vascular grafts with gelatin-sheathed coaxially structured nanofibers. *Langmuir* **2015**, *31* (47), 12993−13002.
(89) Han, J.; Lazarovici, P.; Pomerantz, C.; Chen, X.; Wei, Y.; Lelkes, P. I. Co-electrospun blends of PLGA, gelatin, and elastin as potential nonthrombogenic scaffolds for vascular tissue engineering. *Biomacromolecules* **2011**, *12* (2), 399−408.
(90) Hajiali, H.; Shahgasempour, S.; Naimi-Jamal, M. R.; Peirovi, H. Electrospun PGA/gelatin nanofibrous scaffolds and their potential application in vascular tissue engineering. *Int. J. Nanomed.* **2011**, *6*, 2133.
(91) Johnson, R.; Ding, Y.; Nagiah, N.; Monnet, E.; Tan, W. Coaxially-structured fibres with tailored material properties for vascular graft implant. *Mater. Sci. Eng., Part C* **2019**, *97*, 1−11.
(92) Norouzi, S. K.; Shamloo, A. Bilayered heparinized vascular graft fabricated by combining electrospinning and freeze drying methods. *Mater. Sci. Eng., Part C* **2019**, *94*, 1067−1076.
(93) Chernonosova, V.; Gostev, A.; Murashov, I.; Chelobanov, B.; Karpenko, A.; Laktionov, P. Assessment of Electrospun Pellethane-Based Scaffolds for Vascular Tissue Engineering. *Materials* **2021**, *14* (13), 3678.
(94) Coimbra, P.; Santos, P.; Alves, P.; Miguel, S. P.; Carvalho, M. P.; de Sá, K. D.; Correia, I.; Ferreira, P. Coaxial electrospun PCL/Gelatin-MA fibers as scaffolds for vascular tissue engineering. *Colloids Surf., B* **2017**, *159*, 7−15.
(95) Birer, M.; Acartürk, F. Telmisartan loaded polycaprolactone/gelatin-based electrospun vascular scaffolds. *Int. J. Polym. Mater. Polym. Biomater.* **2021**, 858−873.
(96) Zhao, Q.; Cui, H.; Wang, J.; Chen, H.; Wang, Y.; Zhang, L.; Du, X.; Wang, M. Regulation effects of biomimetic hybrid scaffolds on vascular endothelium remodeling. *ACS Appl. Mater. Interfaces* **2018**, *10* (28), 23583−23594.
(97) Chuang, C.-H.; Lin, R.-Z.; Tien, H.-W.; Chu, Y.-C.; Li, Y.-C.; Melero-Martin, J. M.; Chen, Y.-C. Enzymatic regulation of functional vascular networks using gelatin hydrogels. *Acta Biomater.* **2015**, *19*, 85−99.
(98) Turner, N. J.; Kielty, C. M.; Walker, M. G.; Canfield, A. E. A novel hyaluronan-based biomaterial (Hyaff-11®) as a scaffold for endothelial cells in tissue engineered vascular grafts. *Biomaterials* **2004**, *25* (28), 5955−5964.
(99) Arulmoli, J.; Wright, H. J.; Phan, D. T.T.; Sheth, U.; Que, R. A.; Botten, G. A.; Keating, M.; Botvinick, E. L.; Pathak, M. M.; Zarembinski, T. I.; Yanni, D. S.; Razorenova, O. V.; Hughes, C. C.W.; Flanagan, L. A. Combination scaffolds of salmon fibrin, hyaluronic acid, and laminin for human neural stem cell and vascular tissue engineering. *Acta Biomater.* **2016**, *43*, 122−138.
(100) Ruiz, A.; Flanagan, C. E.; Masters, K. S. Differential support of cell adhesion and growth by copolymers of polyurethane with hyaluronic acid. *J. Biomed. Mater. Res., A* **2013**, *101* (10), 2870−2882.
(101) Necas, J.; Bartosikova, L.; Brauner, P.; Kolar, J. Hyaluronic acid (hyaluronan): a review. *Vet. Med. (Prague, Czech Repub.)* **2008**, *53* (8), 397−411.
(102) Qin, K.; Wang, F.; Simpson, R. M.; Zheng, X.; Wang, H.; Hu, Y.; Gao, Z.; Xu, Q.; Zhao, Q. Hyaluronan promotes the regeneration of vascular smooth muscle with potent contractile function in rapidly biodegradable vascular grafts. *Biomaterials* **2020**, *257*, 120226.
(103) Shojaee, M.; Swaminathan, G.; Bashur, C. A.; Ramamurthi, A. Temporal changes in peritoneal cell phenotype and neoelastic matrix induction with hyaluronan oligomers and TGF-β1 after implantation of engineered conduits. *J.Tissue Eng. Regener. Med.* **2018**, *12* (6), 1420−1431.
(104) Pandis, L.; Zavan, B.; Abatangelo, G.; Lepidi, S.; Cortivo, R.; Vindigni, V. Hyaluronan-based scaffold for in vivo regeneration of the rat vena cava: Preliminary results in an animal model. *J. Biomed. Mater. Res. Part A* **2010**, *93* (4), 1289−1296.
(105) Jia, W.; Li, M.; Kang, L.; Gu, G.; Guo, Z.; Chen, Z. Fabrication and comprehensive characterization of biomimetic extracellular matrix electrospun scaffold for vascular tissue engineering applications. *J. Mater. Sci.* **2019**, *54* (15), 10871−10883.
(106) Dimitrievska, S.; Wang, J.; Lin, T.; Weyers, A.; Bai, H.; Qin, L.; Li, G.; Cai, C.; Kypson, A.; Kristofik, N.; Gard, A.; Sundaram, S.; Yamamoto, K.; Wu, W.; Zhao, L.; Kural, M. H.; Yuan, Y.; Madri, J.; Kyriakides, T. R.; Linhardt, R. J.; Niklason, L. E. Glycocalyx-Like Hydrogel Coatings for Small Diameter Vascular Grafts. *Adv. Funct. Mater.* **2020**, *30* (23), 1908963.
(107) Filová, E.; Brynda, E.; Riedel, T.; Chlupáč, J.; Vandrovcová, M.; Švindrych, Z.; Lisá, V.; Houska, M.; Pirk, J.; Bačáková, L. Improved adhesion and differentiation of endothelial cells on surface-attached fibrin structures containing extracellular matrix proteins. *J. Biomed. Mater. Res. Part A* **2014**, *102* (3), 698−712.

https://doi.org/10.1021/acsomega.2c01740
ACS Omega 2022, 7, 22125−22148

(108) Williams, S. K.; Kleinert, L. B.; Patula-Steinbrenner, V. Accelerated neovascularization and endothelialization of vascular grafts promoted by covalently bound laminin type 1. *J. Biomed. Mater. Res. Part A* **2011**, *99* (1), 67−73.
(109) Yang, L.; Li, X.; Wang, D.; Mu, S.; Lv, W.; Hao, Y.; Lu, X.; Zhang, G.; Nan, W.; Chen, H.; Xie, L.; Zhang, Y.; Dong, Y.; Zhang, Q.; Zhao, L. Improved mechanical properties by modifying fibrin scaffold with PCL and its biocompatibility evaluation. *J. Biomater. Sci. Polym. Ed.* **2020**, *31* (5), 658−678.
(110) Noori, A.; Ashrafi, S. J.; Vaez-Ghaemi, R.; Hatamian-Zaremi, A.; Webster, T. J. A review of fibrin and fibrin composites for bone tissue engineering. *Int. J. Nanomed.* **2017**, *12*, 4937.
(111) Zhang, Q.; Yan, S.; You, R.; Kaplan, D. L.; Liu, Y.; Qu, J.; Li, X.; Li, M.; Wang, X. Multichannel silk protein/laminin grafts for spinal cord injury repair. *J. Biomed. Mater. Res., Part A* **2016**, *104* (12), 3045−3057.
(112) Daum, R.; Visser, D.; Wild, C.; Kutuzova, L.; Schneider, M.; Lorenz, G.; Weiss, M.; Hinderer, S.; Stock, U. A.; Seifert, M.; Schenke-Layland, K. Fibronectin adsorption on electrospun synthetic vascular grafts attracts endothelial progenitor cells and promotes endothelialization in dynamic in vitro culture. *Cells* **2020**, *9* (3), 778.
(113) De Visscher, G.; Mesure, L.; Meuris, B.; Ivanova, A.; Flameng, W. Improved endothelialization and reduced thrombosis by coating a synthetic vascular graft with fibronectin and stem cell homing factor SDF-1α. *Acta Biomater.* **2012**, *8* (3), 1330−1338.
(114) Wang, N.; Zheng, W.; Cheng, S.; Zhang, W.; Liu, S.; Jiang, X. In vitro evaluation of essential mechanical properties and cell behaviors of a novel polylactic-co-glycolic acid (PLGA)-based tubular scaffold for small-diameter vascular tissue engineering. *Polymers* **2017**, *9* (8), 318.
(115) Ye, C.; Wang, Y.; Su, H.; Yang, P.; Huang, N.; Maitz, M. F.; Zhao, A. Construction of a fucoidan/laminin functional multilayer to direction vascular cell fate and promotion hemocompatibility. *Mater. Sci. Eng., Part C* **2016**, *64*, 236−242.
(116) Cordelle, J.; Mantero, S. Insight on the endothelialization of small silk-based tissue-engineered vascular grafts. *Int. J. Artif. Organs* **2020**, *43* (10), 631−644.
(117) Kiritani, S.; Kaneko, J.; Ito, D.; Morito, M.; Ishizawa, T.; Akamatsu, N.; Tanaka, M.; Iida, T.; Tanaka, T.; Tanaka, R.; Asakura, T.; Arita, J.; Hasegawa, K. Silk fibroin vascular graft: a promising tissue-engineered scaffold material for abdominal venous system replacement. *Sci. Rep.* **2020**, *10* (1), 21041.
(118) Obiweluozor, F. O.; Emechebe, G. A.; Kim, D.-W.; Cho, H.-J.; Park, C. H.; Kim, C. S.; Jeong, I. S. Considerations in the development of small-diameter vascular graft as an alternative for bypass and reconstructive surgeries: A review. *Cardiovasc. Eng. Technol.* **2020**, *11* (5), 495−521.
(119) Fukayama, T.; Ozai, Y.; Shimokawadoko, H.; Aytemiz, D.; Tanaka, R.; Machida, N.; Asakura, T. Effect of fibroin sponge coating on in vivo performance of knitted silk small diameter vascular grafts. *Organogenesis* **2015**, *11* (3), 137−151.
(120) Rodriguez, M.; Kluge, J. A.; Smoot, D.; Kluge, M. A.; Schmidt, D. F.; Paetsch, C. R.; Kim, P. S.; Kaplan, D. L. Fabricating mechanically improved silk-based vascular grafts by solution control of the gel-spinning process. *Biomaterials* **2020**, *230*, 119567.
(121) Tanaka, K.; Fukuda, D.; Higashikuni, Y.; Hirata, Y.; Komuro, I.; Saotome, T.; Yamashita, Y.; Asakura, T.; Sata, M. Biodegradable extremely-small-diameter vascular graft made of silk fibroin can be implanted in mice. *J. Atheroscler. Thromb.* **2020**, *27*, 1299−1309.
(122) Liu, S.; Dong, C.; Lu, G.; Lu, Q.; Li, Z.; Kaplan, D. L.; Zhu, H. Bilayered vascular grafts based on silk proteins. *Acta Biomater.* **2013**, *9* (11), 8991−9003.
(123) Aussel, A; Thebaud, N B; Berard, X; Brizzi, V; Delmond, S; Bareille, R; Siadous, R; James, C; Ripoche, J; Durand, M; Montembault, A; Burdin, B; Letourneur, D; L'Heureux, N; David, L; Bordenave, L Chitosan-based hydrogels for developing a small-diameter vascular graft: in vitro and in vivo evaluation. *Biomed. Mater.* **2017**, *12* (6), 065003.
(124) Yao, Y.; Wang, J.; Cui, Y.; Xu, R.; Wang, Z.; Zhang, J.; Wang, K.; Li, Y.; Zhao, Q.; Kong, D. Effect of sustained heparin release from PCL/chitosan hybrid small-diameter vascular grafts on anti-thrombogenic property and endothelialization. *Acta Biomater.* **2014**, *10* (6), 2739−2749.
(125) Spadaccio, C.; Chello, M.; Trombetta, M.; Rainer, A.; Toyoda, Y.; Genovese, J. A. Drug releasing systems in cardiovascular tissue engineering. *J. Cell. Mol. Med.* **2009**, *13* (3), 422−439.
(126) Wang, Y.; Ma, B.; Yin, A.; Zhang, B.; Luo, R.; Pan, J.; Wang, Y. Polycaprolactone vascular graft with epigallocatechin gallate embedded sandwiched layer-by-layer functionalization for enhanced antithrombogenicity and anti-inflammation. *J. Controlled Release* **2020**, *320*, 226−238.
(127) Tatterton, M.; Wilshaw, S.-P.; Ingham, E.; Homer-Vanniasinkam, S. The use of antithrombotic therapies in reducing synthetic small-diameter vascular graft thrombosis. *Vasc. Endovasc. Surg.* **2012**, *46* (3), 212−222.
(128) Saitow, C.; Kaplan, D. L.; Castellot Jr, J. J. Heparin stimulates elastogenesis: application to silk-based vascular grafts. *Matrix Biol.* **2011**, *30* (5−6), 346−355.
(129) Jin, X.; Geng, X.; Jia, L.; Xu, Z.; Ye, L.; Gu, Y.; Zhang, A. Y.; Feng, Z. G. Preparation of small-diameter tissue-engineered vascular grafts electrospun from heparin end-capped PCL and evaluation in a rabbit carotid artery replacement model. *Macromol. Biosci.* **2019**, *19* (8), 1900114.
(130) Matsuzaki, Y.; Ulziibayar, A.; Shoji, T.; Shinoka, T. Heparin-Eluting Tissue-Engineered Bioabsorbable Vascular Grafts. *Appl. Sci.* **2021**, *11* (10), 4563.
(131) Wang, D.; Wang, X.; Zhang, Z.; Wang, L.; Li, X.; Xu, Y.; Ren, C.; Li, Q.; Turng, L.-S. Programmed release of multimodal, cross-linked vascular endothelial growth factor and heparin layers on electrospun polycaprolactone vascular grafts. *ACS Appl. Mater. Interfaces* **2019**, *11* (35), 32533−32542.
(132) Choi, W. S.; Joung, Y. K.; Lee, Y.; Bae, J. W.; Park, H. K.; Park, Y. H.; Park, J.-C.; Park, K. D. Enhanced patency and endothelialization of small-caliber vascular grafts fabricated by coimmobilization of heparin and cell-adhesive peptides. *ACS Appl. Mater. Interfaces* **2016**, *8* (7), 4336−4346.
(133) Kabirian, F.; Brouki Milan, P.; Zamanian, A.; Heying, R.; Mozafari, M. Nitric oxide-releasing vascular grafts: A therapeutic strategy to promote angiogenic activity and endothelium regeneration. *Acta Biomater.* **2019**, *92*, 82−91.
(134) de Mel, A.; Murad, F.; Seifalian, A. M. Nitric oxide: a guardian for vascular grafts? *Chem. Rev.* **2011**, *111* (9), 5742−5767.
(135) Enayati, M.; Schneider, K. H.; Almeria, C.; Grasl, C.; Kaun, C.; Messner, B.; Rohringer, S.; Walter, I.; Wojta, J.; Budinsky, L.; Walpoth, B. H.; Schima, H.; Kager, G.; Hallstrom, S.; Podesser, B. K.; Bergmeister, H. S-nitroso human serum albumin as a nitric oxide donor in drug-eluting vascular grafts: Biofunctionality and preclinical evaluation. *Acta Biomater.* **2021**, *134*, 276−288.
(136) Zhang, X.; Wang, Y.; Liu, J.; Shi, J.; Mao, D.; Midgley, A. C.; Leng, X.; Kong, D.; Wang, Z.; Liu, B.; Wang, S. A metal-organic-framework incorporated vascular graft for sustained nitric oxide generation and long-term vascular patency. *Chem. Eng. J.* **2021**, *421*, 129577.
(137) Wang, L.; Xin, X.; Li, P.; Dou, J.; Han, X.; Shen, J.; Yuan, J. Stepwise immobilization of keratin-dopamine conjugates and gold nanoparticles on PET sheets for potential vascular graft with the catalytic generation of nitric oxide. *Colloids Surf., B* **2021**, *205*, 111855.
(138) Naghavi, N.; Seifalian, A. M.; Hamilton, G.; de Mel, A. Evaluation of experimental methods for nitric oxide release from cardiovascular implants; bypass grafts as an exemplar. *Ther. Adv. Cardiovasc. Dis.* **2015**, *9* (6), 375−388.
(139) Yao, Y.; Yim, E. K. Fucoidan for cardiovascular application and the factors mediating its activities. *Carbohydr. Polym.* **2021**, *270*, 118347. Vesel, A.; Mozetic, M.; Strnad, S. Improvement of adhesion of fucoidan on polyethylene terephthalate surface using gas plasma treatments. *Vacuum* **2011**, *85* (12), 1083−1086.

https://doi.org/10.1021/acsomega.2c01740
ACS Omega 2022, 7, 22125−22148

(140) Yao, Y.; Zaw, A. M.; Anderson, D. E.; Hinds, M. T.; Yim, E. K. Fucoidan functionalization on poly (vinyl alcohol) hydrogels for improved endothelialization and hemocompatibility. *Biomaterials* **2020**, *249*, 120011.
(141) Alexandre, N.; Amorim, I.; Caseiro, A. R.; Pereira, T.; Alvites, R.; Rêma, A.; Gonçalves, A.; Valadares, G.; Costa, E.; Santos-Silva, A. Long term performance evaluation of small-diameter vascular grafts based on polyvinyl alcohol hydrogel and dextran and MSCs-based therapies using the ovine pre-clinical animal model. *Int. J. Pharm. (Amsterdam, Neth.)* **2016**, *513*, 332−346.
(142) Zare, M.; Bigham, A.; Zare, M.; Luo, H.; Rezvani Ghomi, E.; Ramakrishna, S. pHEMA: An overview for biomedical applications. *Int. J. Mol. Sci.* **2021**, *22* (12), 6376.
(143) Ji, Y.; Wei, Y.; Liu, X.; Wang, J.; Ren, K.; Ji, J. Zwitterionic polycarboxybetaine coating functionalized with REDV peptide to improve selectivity for endothelial cells. *J. Biomed. Mater. Res. Part A* **2012**, *100* (6), 1387−1397.
(144) Rychter, M.; Milanowski, B.; Grześkowiak, B. F.; Jarek, M.; Kempiński, M.; Coy, E. L.; Borysiak, S.; Baranowska-Korczyc, A.; Lulek, J. Cilostazol-loaded electrospun three-dimensional systems for potential cardiovascular application: Effect of fibers hydrophilization on drug release, and cytocompatibility. *J. Colloid Interface Sci.* **2019**, *536*, 310−327.
(145) Del Gaudio, C.; Ercolani, E.; Galloni, P.; Santilli, F.; Baiguera, S.; Polizzi, L.; Bianco, A. Aspirin-loaded electrospun poly (ε-caprolactone) tubular scaffolds: potential small-diameter vascular grafts for thrombosis prevention. *J. Mater. Sci. Mater. Med.* **2013**, *24* (2), 523−532.
(146) Punnakitikashem, P.; Truong, D.; Menon, J. U.; Nguyen, K. T.; Hong, Y. Electrospun biodegradable elastic polyurethane scaffolds with dipyridamole release for small diameter vascular grafts. *Acta Biomater.* **2014**, *10* (11), 4618−4628.
(147) Detta, N.; Errico, C.; Dinucci, D.; Puppi, D.; Clarke, D. A.; Reilly, G. C.; Chiellini, F. Novel electrospun polyurethane/gelatin composite meshes for vascular grafts. *J. Mater. Sci.: Mater. Medicine* **2010**, *21* (5), 1761−1769.
(148) Shi, J.; Chen, S.; Wang, L.; Zhang, X.; Gao, J.; Jiang, L.; Tang, D.; Zhang, L.; Midgley, A.; Kong, D.; Wang, S. Rapid endothelialization and controlled smooth muscle regeneration by electrospun heparin-loaded polycaprolactone/gelatin hybrid vascular grafts. *J. Biomed. Mater. Res. Part B* **2019**, *107* (6), 2040−2049.
(149) Xing, Y.; Gu, Y.; Guo, L.; Guo, J.; Xu, Z.; Xiao, Y.; Fang, Z.; Wang, C.; Feng, Z.-G.; Wang, Z. Gelatin coating promotes in situ endothelialization of electrospun polycaprolactone vascular grafts. *J. Biomater. Sci., Polym. Ed.* **2021**, *32* (9), 1161−1181.
(150) Browning, M.B.; Dempsey, D.; Guiza, V.; Becerra, S.; Rivera, J.; Russell, B.; Hook, M.; Clubb, F.; Miller, M.; Fossum, T.; Dong, J.F.; Bergeron, A.L.; Hahn, M.; Cosgriff-Hernandez, E. Multilayer vascular grafts based on collagen-mimetic proteins. *Acta Biomater.* **2012**, *8* (3), 1010−1021.
(151) Kudryavtseva, V.; Stankevich, K.; Kozelskaya, A.; Kibler, E.; Zhukov, Y.; Malashicheva, A.; Golovkin, A.; Mishanin, A.; Filimonov, V.; Bolbasov, E.; Tverdokhlebov, S. Magnetron plasma mediated immobilization of hyaluronic acid for the development of functional double-sided biodegradable vascular graft. *Appl. Surf. Sci.* **2020**, *529*, 147196.
(152) Chuang, T.-W.; Masters, K. S. Regulation of polyurethane hemocompatibility and endothelialization by tethered hyaluronic acid oligosaccharides. *Biomaterials* **2009**, *30* (29), 5341−5351.
(153) Ruiz, A.; Rathnam, K. R.; Masters, K. S. Effect of hyaluronic acid incorporation method on the stability and biological properties of polyurethane-hyaluronic acid biomaterials. *J. Mater. Sci.: Mater. Med.* **2014**, *25* (2), 487−498.
(154) Yu, C.; Guan, G.; Glas, S.; Wang, L.; Li, Z.; Turng, L.-S. A biomimetic basement membrane consisted of hybrid aligned nanofibers and microfibers with immobilized collagen IV and laminin for rapid endothelialization. *Bio-Des. Manuf.* **2021**, *4* (2), 171−189.
(155) Zhao, L.; Li, X.; Yang, L.; Sun, L.; Mu, S.; Zong, H.; Li, Q.; Wang, F.; Song, S.; Yang, C.; Zhao, C.; Chen, H.; Zhang, R.; Wang, S.; Dong, Y.; Zhang, Q. Evaluation of remodeling and regeneration of electrospun PCL/fibrin vascular grafts in vivo. *Mater. Sci. Eng., C* **2021**, *118*, 111441.
(156) Woods, I.; Black, A.; Molloy, E. J.; Jockenhoevel, S.; Flanagan, T. C. Fabrication of blood-derived elastogenic vascular grafts using electrospun fibrinogen and polycaprolactone composite scaffolds for paediatric applications. *J. Tissue Eng. Regener. Med.* **2020**, *14* (9), 1281−1295.
(157) Wacker, M.; Riedel, J.; Walles, H.; Scherner, M.; Awad, G.; Varghese, S.; Schurlein, S.; Garke, B.; Veluswamy, P.; Wippermann, J.; Hulsmann, J. Comparative Evaluation on Impacts of Fibronectin, Heparin-Chitosan, and Albumin Coating of Bacterial Nanocellulose Small-Diameter Vascular Grafts on Endothelialization In Vitro. *Nanomaterials* **2021**, *11* (8), 1952.
(158) Sultana, T.; Amirian, J.; Park, C.; Lee, S. J.; Lee, B.-T. Preparation and characterization of polycaprolactone-polyethylene glycol methyl ether and polycaprolactone-chitosan electrospun mats potential for vascular tissue engineering. *J. Biomater. Appl.* **2017**, *32* (5), 648−662.
(159) Maleki, S.; Shamloo, A.; Kalantarnia, F. Tubular TPU/SF nanofibers covered with chitosan-based hydrogels as small-diameter vascular grafts with enhanced mechanical properties. *Sci. Rep.* **2022**, *12* (1), 6179.
(160) Subramaniam, R.; Mani, M. P.; Jaganathan, S. K. Fabrication and testing of electrospun polyurethane blended with chitosan nanoparticles for vascular graft applications. *Cardiovasc. Eng. Technol.* **2018**, *9* (3), 503−513.
(161) Fukunishi, T.; Best, C. A.; Sugiura, T.; Shoji, T.; Yi, T.; Udelsman, B.; Ohst, D.; Ong, C. S.; Zhang, H.; Shinoka, T.; Breuer, C. K.; Johnson, J.; Hibino, N. Tissue-engineered small diameter arterial vascular grafts from cell-free nanofiber PCL/chitosan scaffolds in a sheep model. *PLoS one* **2016**, *11* (7), No. e0158555.
(162) Tanaka, T.; Tanaka, R.; Ogawa, Y.; Takagi, Y.; Sata, M.; Asakura, T. Evaluation of small-diameter silk vascular grafts implanted in dogs. *JTCVS Open* **2021**, *6*, 148−156.
(163) Alessandrino, A.; Chiarini, A.; Biagiotti, M.; Dal Prà, I.; Bassani, G. A.; Vincoli, V.; Settembrini, P.; Pierimarchi, P.; Freddi, G.; Armato, U. Three-layered silk fibroin tubular scaffold for the repair and regeneration of small caliber blood vessels: from design to in vivo pilot tests. *Front. Bioeng. Biotechnol.* **2019**, *7*, 356.
(164) Yin, A.; Zhang, K.; McClure, M. J.; Huang, C.; Wu, J.; Fang, J.; Mo, X.; Bowlin, G. L.; Al-Deyab, S. S.; El-Newehy, M. Electrospinning collagen/chitosan/poly (L-lactic acid-co-ε-caprolactone) to form a vascular graft: Mechanical and biological characterization. *J. Biomed. Mater. Res., Part A* **2013**, *101* (5), 1292−1301.
(165) Dong, X.; Yuan, X.; Wang, L.; Liu, J.; Midgley, A. C.; Wang, Z.; Wang, K.; Liu, J.; Zhu, M.; Kong, D. Construction of a bilayered vascular graft with smooth internal surface for improved hemocompatibility and endothelial cell monolayer formation. *Biomaterials* **2018**, *181*, 1−14.
(166) Wang, Z.; Liu, C.; Zhu, D.; Gu, X.; Xu, Y.; Qin, Q.; Dong, N.; Zhang, S.; Wang, J. Untangling the co-effects of oriented nanotopography and sustained anticoagulation in a biomimetic intima on neovessel remodeling. *Biomaterials* **2020**, *231*, 119654.
(167) Huang, R.; Gao, X.; Wang, J.; Chen, H.; Tong, C.; Tan, Y.; Tan, Z. Triple-layer vascular grafts fabricated by combined E-jet 3D printing and electrospinning. *Ann. Biomed. Eng.* **2018**, *46* (9), 1254−1266.
(168) Gostev, A. A.; Chernonosova, V. S.; Murashov, I. S.; Sergeevichev, D. S.; Korobeinikov, A. A.; Karaskov, A. M.; Karpenko, A. A.; Laktionov, P. P. Electrospun polyurethane-based vascular grafts: physicochemical properties and functioning in vivo. *Biomed. Mater.* **2020**, *15* (1), 015010.
(169) Bergmeister, H.; Schreiber, C.; Grasl, C.; Walter, I.; Plasenzotti, R.; Stoiber, M.; Bernhard, D.; Schima, H. Healing characteristics of electrospun polyurethane grafts with various porosities. *Acta Biomater.* **2013**, *9* (4), 6032−6040.
(170) Soliman, S.; Sant, S.; Nichol, J. W.; Khabiry, M.; Traversa, E.; Khademhosseini, A. Controlling the porosity of fibrous scaffolds by

https://doi.org/10.1021/acsomega.2c01740
ACS Omega 2022, 7, 22125−22148

modulating the fiber diameter and packing density. *J. Biomed. Mater. Res. Part A* **2011**, *96* (3), 566−574.
(171) De Valence, S.; Tille, J.-C.; Giliberto, J.-P.; Mrowczynski, W.; Gurny, R.; Walpoth, B.; Möller, M. Advantages of bilayered vascular grafts for surgical applicability and tissue regeneration. *Acta Biomater.* **2012**, *8* (11), 3914−3920.
(172) Xing, M.-y.; Yu, C.-l.; Wu, Y.-f.; Wang, L.; Guan, G.-p. Preparation and characterization of a polyvinyl alcohol/polyacrylamide hydrogel vascular graft reinforced with a braided fiber stent. *Text. Res. J.* **2020**, *90* (13−14), 1537−1548.
(173) Post, A.; Kishan, A. P.; Diaz-Rodriguez, P.; Tuzun, E.; Hahn, M.; Cosgriff-Hernandez, E. Introduction of sacrificial bonds to hydrogels to increase defect tolerance during suturing of multilayer vascular grafts. *Acta Biomater.* **2018**, *69*, 313−322.
(174) Zhang, C.; Xie, Q.; Cha, R.; Ding, L.; Jia, L.; Mou, L.; Cheng, S.; Wang, N.; Li, Z.; Sun, Y.; Cui, C.; Zhang, Y.; Zhang, Y.; Zhou, F.; Jiang, X. Anticoagulant Hydrogel Tubes with Poly (ε-Caprolactone) Sheaths for Small-Diameter Vascular Grafts. *Adv. Healthcare Mater.* **2021**, *10*, 2100839.
(175) Cutiongco, M. F.; Anderson, D. E.; Hinds, M. T.; Yim, E. K. In vitro and ex vivo hemocompatibility of off-the-shelf modified poly (vinyl alcohol) vascular grafts. *Acta Biomater.* **2015**, *25*, 97−108.
(176) Khodadoust, M.; Mohebbi-Kalhori, D.; Jirofti, N. Fabrication and characterization of electrospun Bi-hybrid PU/PET scaffolds for small-diameter vascular grafts applications. *Cardiovasc. Eng. Technol.* **2018**, *9* (1), 73−83.
(177) Kharazi, A. Z.; Atari, M.; Vatankhah, E.; Javanmard, S. H. A nanofibrous bilayered scaffold for tissue engineering of small-diameter blood vessels. *Polym. Adv. Technol.* **2018**, *29* (12), 3151−3158.
(178) Elsayed, Y.; Lekakou, C.; Labeed, F.; Tomlins, P. Fabrication and characterisation of biomimetic, electrospun gelatin fibre scaffolds for tunica media-equivalent, tissue engineered vascular grafts. *Mater. Sci. Eng.: C* **2016**, *61*, 473−483.
(179) Wang, W.; Nie, W.; Zhou, X.; Feng, W.; Chen, L.; Zhang, Q.; You, Z.; Shi, Q.; Peng, C.; He, C. Fabrication of heterogeneous porous bilayered nanofibrous vascular grafts by two-step phase separation technique. *Acta Biomater.* **2018**, *79*, 168−181.
(180) Gupta, P.; Lorentz, K. L.; Haskett, D. G.; Cunnane, E. M.; Ramaswamy, A. K.; Weinbaum, J. S.; Vorp, D. A.; Mandal, B. B. Bioresorbable silk grafts for small diameter vascular tissue engineering applications: In vitro and in vivo functional analysis. *Acta Biomater.* **2020**, *105*, 146−158.
(181) Dempsey, D. K.; Nezarati, R. M.; Mackey, C. E.; Cosgriff-Hernandez, E. M. High Compliance Vascular Grafts Based on Semi-Interpenetrating Networks. *Macromol. Mater. Eng.* **2014**, *299* (12), 1455−1464.
(182) Byrne, O.; Coulter, F.; Roche, E. T.; O'Cearbhaill, E. D. In silico design of additively manufacturable composite synthetic vascular conduits and grafts with tuneable compliance. *Biomater. Sci.* **2021**, *9*, 4343.
(183) Loewen, A.; Kossel, K.-M.; Gesché, V.; Gries, T.; Jockenhoevel, S. Combining material and structural elasticity-An approach to enhanced compliance of small-calibre vascular grafts. *IOP Conf. Ser.: Mater. Sci. Eng.* **2017**, *254*, 062007.
(184) Filipe, E. C.; Santos, M.; Hung, J.; Lee, B. S.; Yang, N.; Chan, A. H.; Ng, M. K.; Rnjak-Kovacina, J.; Wise, S. G. Rapid endothelialization of off-the-shelf small diameter silk vascular grafts. *Pain. Genet.* **2018**, *3* (1), 38−53.
(185) Tanaka, T.; Tanaka, R.; Ogawa, Y.; Takagi, Y.; Sata, M.; Asakura, T. Evaluation of small-diameter silk vascular grafts implanted in dogs. *JTCVS Open* **2021**, *6*, 148.
(186) Ahn, C. B.; Kim, J. H.; Lee, J.-H.; Park, K. Y.; Son, K. H.; Lee, J. W. Development of Multi-layer Tubular Vascular Scaffold to Enhance Compliance by Exhibiting a Negative Poisson's Ratio. *Int. J. Prec. Eng.Manuf.* **2021**, *8* (3), 841−853.
(187) Furdella, K. J.; Higuchi, S.; Behrangzade, A.; Kim, K.; Wagner, W. R.; Vande Geest, J. P. In-vivo assessment of a tissue engineered vascular graft computationally optimized for target vessel compliance. *Acta Biomater.* **2021**, *123*, 298−311.
(188) Zhang, Y; Li, X S; Guex, A G; Liu, S S; Muller, E; Malini, R I.; Zhao, H J; Rottmar, M; Maniura-Weber, K; Rossi, R M; Spano, F A compliant and biomimetic three-layered vascular graft for small blood vessels. *Biofabrication* **2017**, *9* (2), 025010.
(189) Kim, S.-H.; Chung, E.; Kim, S.-H.; Jung, Y.; Kim, Y. H.; Kim, S. H. A novel seamless elastic scaffold for vascular tissue engineering. *J. Biomater. Sci., Polym. Ed.* **2010**, *21* (3), 289−302.
(190) Zbinden, J. C.; Blum, K. M.; Berman, A. G.; Ramachandra, A. B.; Szafron, J. M.; Kerr, K. E.; Anderson, J. L.; Sangha, G. S.; Earl, C. C.; Nigh, N. R.; Mirhaidari, G. J. M.; Reinhardt, J. W.; Chang, Y.-C.; Yi, T.; Smalley, R.; Gabriele, P. D.; Harris, J. J.; Humphrey, J. D.; Goergen, C. J.; Breuer, C. K. Effects of Braiding Parameters on Tissue Engineered Vascular Graft Development. *Adv. Healthcare Mater.* **2020**, *9* (24), 2001093.
(191) Hiob, M. A.; She, S.; Muiznieks, L. D.; Weiss, A. S. Biomaterials and modifications in the development of small-diameter vascular grafts. *ACS Biomater. Sci. Eng.* **2017**, *3* (5), 712−723.
(192) Soldani, G.; Losi, P.; Bernabei, M.; Burchielli, S.; Chiappino, D.; Kull, S.; Briganti, E.; Spiller, D. Long term performance of small-diameter vascular grafts made of a poly (ether) urethane-polydimethylsiloxane semi-interpenetrating polymeric network. *Biomaterials* **2010**, *31* (9), 2592−2605.
(193) Caracciolo, P. C.; Diaz-Rodriguez, P.; Ardao, I.; Moreira, D.; Montini-Ballarin, F.; Abraham, G. A.; Concheiro, A.; Alvarez-Lorenzo, C. Evaluation of human umbilical vein endothelial cells growth onto heparin-modified electrospun vascular grafts. *Int. J. Biol. Macromol.* **2021**, *179*, 567−575.
(194) Zhang, B.; Xu, Y.; Ma, S.; Wang, L.; Liu, C.; Xu, W.; Shi, J.; Qiao, W.; Yang, H. Small-diameter polyurethane vascular graft with high strength and excellent compliance. *J. Mech. Behav. Biomed. Mater.* **2021**, *121*, 104614.
(195) Mi, H.-Y.; Jiang, Y.; Jing, X.; Enriquez, E.; Li, H.; Li, Q.; Turng, L.-S. Fabrication of triple-layered vascular grafts composed of silk fibers, polyacrylamide hydrogel, and polyurethane nanofibers with biomimetic mechanical properties. *Mater. Sci. Eng.: C* **2019**, *98*, 241−249.
(196) Stoiber, M.; Grasl, C.; Frieberger, K.; Moscato, F.; Bergmeister, H.; Schima, H. Impact of the testing protocol on the mechanical characterization of small diameter electrospun vascular grafts. *J. Mech. Behav. Biomed. Mater.* **2020**, *104*, 103652.
(197) Yagi, T.; Sato, M.; Nakazawa, Y.; Tanaka, K.; Sata, M.; Itoh, K.; Takagi, Y.; Asakura, T. Preparation of double-raschel knitted silk vascular grafts and evaluation of short-term function in a rat abdominal aorta. *J. Artif. Organs* **2011**, *14* (2), 89−99.
(198) Lores, N. J.; Hung, X.; Talou, M. H.; Abraham, G. A.; Caracciolo, P. C. Novel three-dimensional printing of poly (ester urethane) scaffolds for biomedical applications. *Polym. Adv. Technol.* **2021**, *32*, 3309.
(199) Li, Z.; Li, X.; Xu, T.; Zhang, L. Acellular small-diameter tissue-engineered vascular grafts. *Appl. Sci.* **2019**, *9* (14), 2864.
(200) Chan, A. H. P.; Filipe, E. C.; Tan, R. P.; Santos, M.; Yang, N.; Hung, J.; Feng, J.; Nazir, S.; Benn, A. J.; Ng, M. K. C.; Rnjak-Kovacina, J.; Wise, S. G. Altered processing enhances the efficacy of small-diameter silk fibroin vascular grafts. *Sci. Rep.* **2019**, *9* (1), 17461.

https://doi.org/10.1021/acsomega.2c01740
ACS Omega 2022, 7, 22125−22148